Short Title: Engineering *Synechococcus* sp. PCC 11901

Title: **Engineering the highly productive cyanobacterium *Synechococcus* sp. PCC 11901**

Authors: Angelo J. Victoria[1,2*], Tiago Toscano Selão[3*], José Ángel Moreno-Cabezuelo[4], Lauren A. Mills[4], Grant A. R. Gale[1,2], David J. Lea-Smith[4], Alistair J. McCormick[†,1,2]

[1] Institute of Molecular Plant Sciences, School of Biological Sciences, University of Edinburgh, EH9 3BF, UK.

[2] Centre for Engineering Biology, School of Biological Sciences, University of Edinburgh, EH9 3BF, UK.

[3] Department of Chemical and Environmental Engineering, University of Nottingham, Nottingham NG7 2RD, UK.

[4] School of Biological Sciences, University of East Anglia, Norwich Research Park, Norwich, NR4 7TJ, UK.

Corresponding author: Alistair McCormick, School of Biological Sciences, University of Edinburgh, +44 (0)1316505316, alistair.mccormick@ed.ac.uk

On sentence summary: Genetic parts were characterised in *Synechococcus* sp. PCC 11901, including a tightly regulated inducible promoter system, efficient CRISPRi and a novel markerless Cas12a genome editing approach.

Author Contributions: AJV and TTS designed the study with input from AM and DL-S. AJV, TTS, JAMC and LAM performed experiments. AM and AJV prepared the manuscript with input from GARG, TTS, and DL-S.

ABSTRACT

Synechococcus sp. PCC 11901 (PCC 11901) is a fast-growing marine cyanobacterial strain that has a capacity for sustained biomass accumulation to very high cell densities, comparable to that achieved by commercially relevant heterotrophic organisms. However, genetic tools to engineer PCC 11901 for biotechnology applications are limited. Here we describe a suite of tools based on the CyanoGate MoClo system to unlock the engineering potential of PCC 11901. First, we characterised neutral sites suitable for stable genomic integration that do not affect growth even at high cell densities. Second, we tested a suite of constitutive promoters, terminators, and inducible promoters including a 2,4-diacetylphloroglucinol (DAPG)-inducible PhlF repressor system, which has not previously been demonstrated in cyanobacteria and showed tight regulation and a 228-fold dynamic range of induction. Lastly, we developed a DAPG-inducible dCas9-based CRISPR interference (CRISPRi) system and a modular method to generate markerless mutants using CRISPR-Cas12a. Based on our findings, PCC 11901 is highly responsive to CRISPRi-based repression and showed high efficiencies for single insertion (31-81%) and multiplex double insertion (25%) genome editing with Cas12a. We envision that these tools will lay the foundations for the adoption of PCC 11901 as a robust model strain for engineering biology and green biotechnology.

INTRODUCTION

Climate change has necessitated a global shift towards more sustainable production practices and the building of a bioeconomy centred on Net Zero Carbon policies (*Net Zero Strategy*, 2021). Cyanobacteria are an attractive alternative to heterotrophic microbial bioproduction chassis, such as *Escherichia coli* and yeast, due to their capacity for biology-based carbon capture and utilisation and potential for the production of a wide array of useful chemicals (Zhang et al., 2017; Daneshvar et al., 2022). Unicellular model cyanobacterial strains, such as *Synechocystis* sp. PCC 6803 (hereafter PCC 6803) and *Synechococcus elongatus* PCC 7942, have been investigated as biorefineries for bulk commodity products such as biofuels (Kopka et al., 2017), bioplastics (Khetkorn et al., 2016), natural colourants (Puzorjov et al., 2022) and terpenoids (Rautela and Kumar, 2022), while filamentous strains such as *Arthrospira platensis* have been developed for the production of food and high-value therapeutic antibodies (Jester et al., 2022; Saveria et al., 2022). Nevertheless, slow growth rates and low biomass productivity remain key bottlenecks that limit the economic competitiveness and commercial expansion of cyanobacterial biotechnology (Lea-Smith et al., 2021).

Several fast-growing cyanobacterial strains have been reported that show strong potential for overcoming yield challenges (for recent review see Selão, 2022), including fresh water strains *Synechococcus elongatus* UTEX 2973 (hereafter UTEX 2973) (Yu et al., 2015), *Synechococcus elongatus* PCC 11801 (hereafter PCC 11801) (Jaiswal et al., 2018), *Synechococcus elongatus* PCC 11802 (Jaiswal et al., 2020), and marine strains *Synechococcus* sp. PCC 7002 (hereafter PCC 7002) (Batterton and Van Baalen, 1971) and *Synechococcus* sp. PCC 11901 (hereafter PCC 11901) (Włodarczyk et al., 2020). Marine cyanobacteria are of particular interest as they can utilise sea/brackish water, circumventing the need for freshwater resources (Hitchcock et al., 2020). In contrast to other fast-growing strains, PCC 11901 has an additional capacity for sustained growth to high densities (up to 30 g/L dry cell weight, DCW), similar to the maximum biomass accumulation observed for batch-cultured *E. coli* cultures (24.7 g/L DCW) (Soini et al., 2008). Furthermore, PCC 11901 can tolerate high light intensities (>900 µmol photons m^{-2} s^{-1}), temperatures (up to 43°C), and salinities over 2-fold higher than sea water (Cho et al., 2023). PCC 11901 is amenable to natural transformation and its genome is fully-sequenced (Włodarczyk et al., 2020). PCC 11901 has also been engineered to produce free fatty acids yielding >6 mM (1.5 g L^{-1}), which is comparable to that achieved by similarly engineered heterotrophic organisms (Xiao et al., 2018). The recent isolation of a cobalamin-independent strain of PCC 11901 (*Synechococcus* sp. UTEX 3154) that does not require the addition of vitamin B12 will help reduce scale-up costs (Mills et al., 2022). Together, these qualities make PCC 11901 an attractive model species for fundamental research and biotechnology applications.

In recent years, standardised molecular tools have been developed to help progress synthetic/engineering biology in cyanobacteria, such as the CyanoGate Modular Cloning system (Vasudevan et al., 2019) and the Start-Stop Assembly method (Taylor et al., 2021). Additional advances include the development of self-replicating vectors for extrachromosomal expression (Taton et al., 2014; Opel et al., 2022), recombineering (Jones et al., 2021), genetic circuits (Taton et al., 2017; Zhang et al., 2022), CRISPR interference (CRISPRi) (Yao et al., 2020), and CRISPR-based gene editing tools to reprogram metabolism (Baldanta et al., 2022; Cengic et al., 2022; Wang et al., 2023). Strategies for biocontainment of mutant cyanobacterial strains have also been developed, for example, using inducible kill-switches (Zhou et al., 2019). Nevertheless, such tools are often not readily transferrable between different species, and to date very few engineering approaches have been characterised in PCC 11901. Notably, Mills et al. (2022) recently reported that

PCC 11901 was not compatible with the negative selection markers *sacB* and *codA* used for generating markerless mutants (i.e. a genome-modified mutant that lacks a selective antibiotic resistance cassette) that have key advantages for biotechnology applications (Lea-Smith et al., 2016).

In this study we investigated a broad set of available genetic parts and developed several novel tools for engineering PCC 11901. We tested five putative neutral integration sites to serve as loci for introducing heterologous DNA and explored the amenability of PCC 11901 to transconjugation. We then characterised the functionality of a suite of known and new genetic parts, including the 2,4-diacetylphloroglucinol (DAPG)-inducible PhlF repressor system. Building on this, we developed an inducible CRISPRi gene repression system and a novel hybrid plasmid approach to successfully generate markerless mutants using CRISPR-Cas12a. Together these tools should fast-track the further development of PCC 11901 as a commercially viable chassis strain for cyanobacterial biotechnology.

RESULTS AND DISCUSSION

Identification of robust neutral sites in PCC 11901 suitable for high-density growth

PCC 11901 is naturally transformable but exhibits partial resistance to kanamycin (Włodarczyk et al., 2020). We first tested the susceptibility of PCC 11901 to five common selective antibiotics used to generate marked mutants (**Figure 1A**). We observed that PCC 11901 exhibited partial resistance to kanamycin at 50 µg mL^{-1} and gentamicin at 10 µg mL^{-1}. In contrast, PC11901 was fully susceptible to spectinomycin, erythromycin, and chloramphenicol at all concentrations tested. Previous work has reported that many filamentous and unicellular species have innate resistances to specific antibiotics, including aminoglycosides such as kanamycin and gentamicin (Dias et al., 2015). Aminoglycoside resistance has been attributed to native redox-active compounds such as glutathione in *Synechocystis* sp. PCC 6803 (Cameron and Pakrasi, 2011), and the presence of native resistance genes such as the kanamycin aminoglycoside acetyltransferase homolog recently described in *Arthrospira platensis* (NIES39_D01030, GenBank ID: BAI89523.1) (Jester et al., 2022; Shiraishi and Nishida, 2022), which is a member of the Gcn5-related N-acetyltransferase (GNAT) superfamily (Favrot et al., 2016). A BLAST analysis of the PCC 11901 genome yielded 13 genes belonging to the GNAT family. The closest homolog to BAI89523.1 (FEK30_08270, GenBank ID: QCS49435.1) shared a 33% peptide sequence

identity with similar conserved domains and a coenzyme A binding pocket motif, and thus may account for the partial resistance observed (**Supplementary Figure S1**).

Neutral sites are genomic loci that allow for stable integration of heterologous genes into the genome with no or minimal phenotypic impact. Several neutral sites have been identified in model cyanobacterial species, such as PCC 6803 and PCC 7002 (Pinto et al., 2015; Ruffing et al., 2016; Vogel et al, 2017). However, no neutral sites have yet been characterised in PCC 11901, specifically at the high densities achievable in this strain. We identified five putative neutral site loci in PCC 11901 based on previously identified neutral integration sites in other cyanobacteria and analysis of the PCC 11901 genome. *desB* (FEK_04840) encodes for a putative fatty acid desaturase, which in PCC 7002 is involved in modulating membrane fluidity at temperatures below 22ºC but does not impact growth at 30ºC (Sakamoto et al., 1997; Ruffing et al., 2016). *glgA1* (FEK_14880) encodes for one of two putative glycogen synthase isoforms in PCC 11901, which has previously been characterised as a neutral site in PCC 6803 and PCC 11801 (Sengupta et al., 2020; Mittermair et al., 2021). The loci for *mrr* (FEK30_09380) and *aquI* (FEK30_10065) encode for a putative Type IV restriction endonuclease and a Type II site-specific deoxyribonuclease, respectively, and were selected based on the hypothesis that several endonuclease genes may be redundant for immunity and not essential for growth. Studies in other cyanobacterial strains, such as *Thermosynechococcus elongatus* BP-1 and PCC 6803, have also reported improved transformation efficiencies in nuclease mutants (Kufryk et al., 2002; Iwai et al., 2004). Lastly, we identified an intergenic region of 185 bp between two convergent predicted open reading frames encoding hypothetical proteins (FEK30_11550 and FEK30_11555), which we hypothesised would not contain important regulatory elements. We called this locus neutral site 1 (NS1). Such regions have previously been used successfully as neutral sites in PCC 6803 and other bacterial chassis strains, including *E. coli, Bacillus subtilis* and *Pseudomonas putida* (Bernhards et al., 2022).

To establish and validate the concentrations at which selection can be performed, we chose the putative neutral site *desB*, previously tested in PCC 11901 (Mills et al., 2022), and introduced antibiotic resistance cassettes (AbRs) for each antibiotic via natural transformation (**Figure 1B**). Following three days of growth, we observed hundreds of transformant colonies for each AbR at concentrations of 100 µg mL^{-1} kanamycin, 25 µg mL^{-1} spectinomycin, 50 µg mL^{-1} gentamicin, 1.25 µg mL^{-1} erythromycin, and 5 µg mL^{-1} chloramphenicol, respectively.

Based on the robust susceptibility of PCC 11901 to spectinomycin and previous success with using spectinomycin for selection in model strains (Vasudevan et al., 2019), we next assembled integrative vectors carrying a spectinomycin resistance cassette (SpR) flanked by homologous regions for each of the five target putative neutral sites to facilitate homologous recombination (HR), and transformed these into wild-type PCC 11901 to produce the mutants Δ*mrr*::SpR, Δ*aquI*::SpR, Δ*desB*::SpR, Δ*glgA1*::SpR, and Δ*NS1*::SpR (**Figure 1C**). Remarkably, we observed full segregation for each of the five mutants following a single re-streak from the transformation plates containing 25 µg mL^{-1} spectinomycin (**Supplementary Figure S2**). The segregated mutants were then subjected to a comparative growth analysis to assess the suitability of each putative neutral site. We observed that *mrr* and *aquI* were the best performing neutral sites, with Δ*mrr*::SpR and Δ*aquI*::SpR reaching optical densities similar to wild-type (i.e. OD_{750} > 100). In contrast, Δ*desB*::SpR and Δ*NS1*::SpR grew similarly to wild-type up to OD_{750} ~50, but then growth rates declined, suggesting that these neutral sites should only be used at lower cell densities. The growth rate of Δ*glgA1*::SpR declined from OD_{750} ~20, indicating that *glgA2* is not able to compensate for the loss of *glgA1* as observed in other strains (Sengupta et al., 2020; Mittermair et al., 2021). Notably, all five mutants grew to higher densities compared to wild-type PCC 6803 and PCC 7002. Together, our results show that endonuclease encoding genes are promising targets for identifying additional robust neutral sites in PCC 11901.

PCC 11901 is amenable to conjugation

Delivery of heterologous DNA into genetically tractable cyanobacteria can also be achieved through conjugal transfer or triparental mating using an *E. coli* 'helper' strain with appropriate transmissible plasmids to enable conjugation of mobilizable plasmid vectors, such as RSF1010-based vectors (Gale et al., 2019). As genome integration and segregation are not required, conjugation has proved to be a powerful tool for rapidly testing genetic parts and libraries in several cyanobacterial strains (Bishé et al., 2019; Puzorjov et al., 2021). We sought to determine whether PCC 11901 is amenable to conjugation by introducing the empty RSF1010-based CyanoGate acceptor vectors pPMQAK1-T and pPMQAK1-T-eYFP, previously assembled by Vasudevan et al., (2019), which both contain a kanamycin resistance cassette (KmR) (**Figure 2A**). We initially obtained colonies on selective media containing kanamycin (**Figure 2B**), but subsequently found that a portion of re-streaked colonies exhibited a yellowing or chlorotic phenotype and were unable to survive successive rounds of streaking (**Figure 2C, D**). We hypothesised that the initial colonies were likely

false-positives due to the native kanamycin resistance of PCC 11901 (**Figure 1A, Supplementary Figure S1**). Thus, we constructed new acceptor vectors pPMQSK1-1 and pPMQSK1-T (for level 1 and level T in CyanoGate) that carried SpR, and assembled pPMQSK1-1 vectors carrying either an eYFP (pPMQSK1-1-eYFP) or *Francisella novicida* derived Cas12a (also known as *Fn*Cpf1) expression cassette (pPMQSK1-1-Cas12a). Following conjugal transfer of pPMQSK1-1-based vectors into PCC 11901 we observed no chlorotic phenotypes in any transconjugant strains after re-streaking (**Figure 2D**), demonstrating that spectinomycin allows for robust selection of transconjugants.

We next performed a comparative growth analysis to explore the potential impact of RSF1010-based vectors on high density growth in PCC 11901. We included a stably integrated Δ*mrr*::eYFP mutant for comparison between transconjugants and transformants (pC1.493, **Supplementary Table S2**). The growth of transconjugants with empty acceptor vectors pPMQAK1-T or pPMQSK1-1 were not significantly different to wild-type PCC 11901 and Δ*mrr*::eYFP (**Figure 2E**). However, growth was reduced in transconjugants with pPMQAK1-T-eYFP, pPMQSK1-1-eYFP or pPMQSK1-1-Cas12a, suggesting that the expression of genes from RSF1010-based vectors could represent a metabolic burden for PCC 11901, at least at high cell densities (Meyer, 2009). A comparison of eYFP fluorescence levels between Δ*mrr*::eYFP and the transconjugants with pPMQAK1-T-eYFP or pPMQSK1-1-eYFP showed that eYFP expression was 50 ± 1% lower in both transconjugants compared to the stable integration mutant (**Figure 2F-G**). Overall, our results show for the first time that conjugation is feasible in PCC 11901. However, for this species the speed of transformation and segregation for genome integration appears more rapid than using conjugation. Furthermore, protein expression levels in stable mutants exceeded transconjugants with RSF1010-based vectors (at least for eYFP), suggesting that stable integration may be the favoured engineering choice in PCC 11901. Nevertheless, the capacity to maintain self-replicating vectors in PCC 11901 could still greatly facilitate the characterisation of genetic parts, an important aspect of strain engineering, and facilitate transient gene expression.

Characterisation of constitutive promoters and transcriptional terminators in PCC 11901

Constitutive promoters provide a stable level of gene expression and are essential parts in the engineering toolbox of any chassis strain. Thus, we characterised a suite of 12 constitutive

promoters derived from Vasudevan et al. (2019) to provide a promoter library with varying strengths for use in engineering PCC 11901. Included were constitutive promoters from PCC 6803 (P_{cpc560} and P_{psbA2L}) and synthetic promoters (P_{J23119}, P_{J23115}, P_{J23113}, P_{J23111}, P_{J23110}, P_{J23103}, P_{J23101}, P_{V02}, P_{V07} and P_{trc10}). Promoter strengths were assessed as expression cassettes driving eYFP through stable genomic integration at the *mrr* neutral site, or on the self-replicating RSF1010-based vector pPMQAK1-T. We were successful in assembling and characterising all 12 constitutive promoters following conjugation using pPMQAK1-T (**Figure 3A**). We were also able to generate and characterise 10 segregated integrative transformants at the *mrr* neutral site (**Figure 3B**). Unfortunately, we were not able to generate transformant colonies for P_{J23119} and P_{trc10} despite multiple attempts. Overall, the three strongest constitutive promoters were P_{cpc560}, P_{J23119}, P_{psbA2L}, which is consistent with findings in other cyanobacterial species (Li et al., 2018; Vasudevan et al., 2019; Sengupta et al., 2020). The PCC 6803 *cpc* operon promoter (P_{cpc560}) was used to drive high expression levels of heterologous genes in several model species, including PCC 6803 and PCC 7002. The P_{psbA2L} promoter drives expression of the photosystem II reaction centre subunit D1. The high light levels used to grow PCC 11901 may support the strong levels of expression seen with P_{psbA2L}, similar to previous work in PCC 6803 and UTEX 2973 under high light conditions (Lindberg et al., 2010; Sakurai et al., 2012; Li et al., 2018). Although the observed trend in promoter strength showed a strong correlation ($R^2 = 0.95$) between those integrated at *mrr* and on pPMQAK1-T (**Figure 3C**), we found that genomic integration resulted in a 32% mean increase in eYFP expression for each promoter over those from RSF1010-based vectors. Previous work in PCC 6803 has observed contrasting results, with promoters on RSF1010-based vectors achieving a 3-fold higher level of expression compared to neutral site integrations (Ng et al., 2015). The latter finding was attributed to an increased plasmid copy-number for the RSF1010-based vector compared to the native chromosome. Thus, in PCC 11901 the copy number ratio may be lower for RSF1010-based vectors relative to the native chromosomes. The chromosomal copy number for PCC 11901 remains unclear and should be a focus for further work.

We next characterised the efficiencies of a suite of 10 transcriptional terminators in PCC 11901 based on those previously characterised in PCC 6803, UTEX 2973 and *E. coli* by Gale et al. (2021). Cyanobacteria rely on the mechanism of rho-independent transcription termination or intrinsic termination, which is defined by the formation of a hairpin loop on the terminator sequence that leads to dissociation of the RNA polymerase and release of the

mRNA transcript (Wilson and von Hippel, 1995). Our suite of intrinsic terminators included six native terminators from *E. coli* ($T_{ECK120010850}$, $T_{ECK120033736}$, $T_{ECK120029600}$, T_{bba_B0011}, T_{bba_B0061}, and T_{rrnB}), two synthetic terminators derived from *E. coli* sequences ($T_{L3S2P21}$ and $T_{L3S2P11}$), and two native terminators from PCC 6803 from photosystem II subunit D1 (T_{psbA2}) and photosystem I subunit B (T_{psaB}) (Chen et al., 2013; Liu & Pakrasi, 2018). Of these, six had termination efficiency (TE) values of >95%, with highest and lowest TE values observed for $T_{ECK120029600}$ (99.8%) and T_{bba_B0061} (47.8%), respectively (**Figure 3D**). Our results were relatively consistent with those from PCC 6803 and UTEX 2973, supporting our previous observation that these transcriptional terminators perform similarly across different cyanobacterial chassis (Gale et al., 2021).

Inducible gene expression systems in PCC 11901

Chemically inducible promoters can be used to modulate gene expression in response to an external stimulus and are powerful tools for fundamental research and advanced engineering approaches (e.g. gene circuit assembly) (Meyer et al., 2019). We first tested the L-rhamnose inducible promoter P_{rhaBAD} and its cognate transcription factor, RhaS, which has previously been characterised in PCC 6803 (Kelly et al., 2018; Behle et al., 2020). To evaluate this system in PCC 11901, we initially investigated if L-rhamnose impacted the growth of wild-type PCC 11901 over a 72 h growth period. We found that PCC 11901 growth was not affected by concentrations of up to 20 mM L-rhamnose, which was twice the highest concentration tested by Behle et al. (2020), suggesting that L-rhamnose is not toxic to PCC 11901 (**Supplementary Figure S3A**). We then constructed an RSF1010-based reporter system RhaS/P_{rhaBAD}-*eYFP*-T_{rrnB} in the pPMQAK1-T vector, using the medium strength constitutive promoter P_{J23101} to drive RhaS expression and eYFP as the fluorescent reporter (**Figure 4A**). Following successful conjugal transfer into PCC 11901, cultures were induced with increasing concentrations of L-rhamnose (0-20 mM) and eYFP fluorescence was measured after 24 h (**Figure 4B**). In the uninduced state (0 mM L-rhamnose), a low level of eYFP fluorescence was detected (305 ± 9 AU, 6.4% of the maximum expression level), demonstrating that the P_{rhaBAD} promoter was leaky. Upon induction, we found that the promoter achieved maximum expression (4,776 ± 185 AU) with 10 mM L-rhamnose, giving a 15-fold dynamic range. Leaky expression with the P_{rhaBAD} promoter has been reported previously in PCC 6803 (Liu et al., 2020). Those authors successfully increased the control of expression by replacing the promoter ribosome binding site with a theophylline riboswitch, although their system required two small molecules for induction.

RNA riboswitches are structured noncoding RNA domains that can regulate gene expression and exert translational control in bacteria by binding small molecules (Kavita and Breaker, 2023). We tested the engineered theophylline-inducible riboswitch E* fused to the *trc* promoter (P_{trc}) first demonstrated in PCC 7942 (Nakahira et al., 2013). We observed that growth of wild-type PCC 11901 was not affected at concentrations up to 2 mM theophylline but was reduced at 5 mM (**Supplementary Figure S3B**). This is consistent with reports in other cyanobacteria of the negative impact of theophylline on growth at concentrations above 2 mM (Ma et al., 2014). We then assembled an RSF1010-based reporter harbouring P_{trcE*}-*eYFP*-T_{rrnB} in the pPMQAK1-T vector for conjugal transfer into PCC1901 (**Figure 4C**). In the absence of theophylline, an eYFP fluorescence signal above background levels was still detected in conjugant strains (336 ± 163.38 AU, 4.8% of the maximum expression level), indicating that P_{trcE*} was leaky in PCC 11901, similar to P_{rhaBAD} (**Figure 4D**). Maximum eYFP expression (8,555 ± 315 AU) was achieved with 2 mM theophylline (giving a 25-fold dynamic range), but expression levels decreased at 5 mM theophylline, likely due to growth inhibition. The observed leaky expression with P_{trcE*} was consistent with reports in several other cyanobacterial species (Taton et al., 2017; Chi et al., 2019).

We sought to identify an inducible system for PCC 11901 that has tighter regulation than the P_{rhaBAD} and P_{trcE*} promoters, so we next evaluated the 2,4-diacetylphloroglucinol (DAPG)-inducible promoter P_{phlF} and its cognate transcription factor PhlF, which has tight regulation in *E. coli* but has not yet been characterised in cyanobacteria (Meyer et al., 2019). In contrast to the RhaS/P_{rhaBAD} system, the PhlF transcription factor functions as a repressor to the P_{phlF} promoter, which undergoes a conformational change upon binding to DAPG and releases the promoter leading to transcription, similar to the TetR family of repressors (Abbas et al., 2002). We assembled two pPMQAK1-T vectors with i) a no TF control harbouring the expression cassette PhlF/P_{phlF}-*eYFP*-T_{rrnB} to test the functionality of the P_{phlF} promoter in the absence of the PhlF repressor transcription factor and DAPG, and ii) the reporter system *phlF*/P_{phlF}-*eYFP*-T_{rrnB}, where the medium strength constitutive promoter PJ_{23101} was used to drive PhlF expression (**Figure 4E**). Following conjugation into PCC 11901, we observed robust levels of YFP expression for the P_{phlF} promoter in the no TF control (94% of P_{cpc560}) (**Figure 2F** and **4F**). For the reporter system, increasing levels of eYFP fluorescence was observed with increasing DAPG concentrations, with maximum expression (6,440 ± 279 AU) achieved upon induction with 10 μM DAPG, similar to that for the no TF control. We

observed near background levels for eYFP fluorescence (28 ± 27 AU) in the uninduced state (0 µM DAPG), indicating very tight repression of P_{phlF} by PhlF. We found that DAPG had no impact on the growth of PCC 11901 up to 10 µM, but that growth rates were reduced at 25 µM DAPG, indicating partial toxicity at higher DAPG concentrations (**Supplementary Figure S3C)**. The latter result was not unexpected, as DAPG has been shown to have broad spectrum activity against bacteria and fungi, particularly those pathogenic to plants (Keel, 1992; Julian et al., 2021). To the best of our knowledge this is the first report of the PhlF/P_{phlF} system being successfully utilised in a cyanobacterial strain. Overall, it provided a wide, 228-fold dynamic range of induction in PCC 11901 and showed tight repression in the absence of DAPG.

Gene repression using CRISPRi

CRISPRi is now well established as a powerful tool to explore gene function and pathways in a variety of model cyanobacterial species (Liu et al., 2020; Yao et al., 2020; Dallo et al., 2023). However, the number of characterised induction systems for CRISPRi remains relatively low for cyanobacteria. Many publications utilise the TetR-based anhydrotetracycline (aTc)-inducible promoters (Huang and Lindblad, 2013), but partial leakiness (i.e. transcriptional repression in the absence of the inducer molecule) and the degree of repression of the available systems can limit effective application, depending on the strain used. Furthermore, aTc is photosensitive and degrades rapidly in UV or blue light (Zess et al., 2016), which we believed would be problematic given the light intensities used to culture PCC 11901 for high density growth and exposure to sunlight for outdoor growth.

To alleviate the potential challenge of aTc instability under high light, we sought to develop a robust and tightly regulated inducible dCas9 CRISPRi approach in PCC 11901 by testing our three inducible promoter systems. Using the CyanoGate system, we assembled the dCas9 expression cassettes *rhaS*/P_{rhaBAD}-*dCas9*-T_{rrnB}, P_{trcE*}-*dCas9*-T_{rrnB} and *phlF*/P_{phlF}-*dCas9*-T_{rrnB} in level 1 position 1 (L1P1). In level 1 position 2 (L1P2), we assembled four different single-guide RNA (sgRNA) expression cassettes (P_{trc10_TSS}-sgRNA-sgRNA scaffold) targeting eYFP at four different sequence locations (**Figure 5A**) (Vasudevan et al., 2019). As a control we also assembled a constitutive expression cassette with a low strength synthetic promoter (P_{J23113}-*dCas9*-T_{rrnB}), as previous work has indicated that strong expression of large proteins, such as dCas9, can produce a metabolic burden that negatively impacts growth (Depardieu and Bikard, 2020). L1P1 and L1P2 vectors were then assembled together into the level T

acceptor pUC19-T pCAT.015 vector for subsequent integration into the *desB* neutral site of the Δ*mrr*::eYFP strain.

We initially tested the functionality of dCas9 in PCC 11901 using the weak constitutive promoter P_{J23113}. Following transformation and segregation, we found that only strains carrying both dCas9 and an sgRNA showed a reduction in eYFP fluorescence, which was similar for all four sgRNAs used (52 ± 3.9%) (**Figure 5B**). No significant impacts on growth were observed between strains (**Supplementary Figure S4A**). Although this demonstrated that CRISPRi-dCas9 was functional in PCC 11901, the reductions in eYFP fluorescence were unimpressive, which we attributed to the low strength of the promoter $P_{J23113.}$ Our results are in line with those in PCC 7002 and *E. coli* where weaker promoters driving dCas9 expression resulted in lower repression of the target gene (Gordon et al., 2016; Fontana et al., 2018).

We then tested the three inducible CRISPRi-dCas9 systems by inducing transformed cultures with 10 mM L-rhamnose, 2 mM theophylline, or 10 μM DAPG, respectively, and measured the change in eYFP fluorescence. Leakiness of dCas9 expression was investigated by measuring eYFP fluorescence in the absence of the respective inducer molecules. For the RhaS/P_{rhaBAD} CRISPRi-dCas9 system we observed a 45-58% reduction in eYFP fluorescence in the absence of L-rhamnose (**Figure 5C**), indicative of the P_{rhaBAD} promoter leakiness observed previously (**Figure 4B**). P_{rhaBAD} appeared able to constitutively express dCas9 at similar levels to that of the weak constitutive promoter P_{J23113}. Overall, our results were consistent with the leakiness reported for P_{rhaBAD} when used to express ddCas12a in PCC 6803 (Liu et al., 2020). Induction with L-rhamnose resulted in a 98 ± 1% decrease in eYFP fluorescence for all sgRNAs in the presence of dCas9. The leakiness of the theophylline-inducible P_{trcE*} was also apparent when used to regulate dCas9, showing a 27% reduction in eYFP fluorescence in the absence of theophylline (**Figure 5D**). Induction of dCas9 expression with theophylline resulted in a similar robust decrease in eYFP fluorescence (98 ± 1%). In contrast, cultures transformed with the DAPG-inducible PhlF/P_{phlF} CRISPRi-dCas9 system showed no reductions in eYFP fluorescence in the absence of DAPG, while the addition of DAPG resulted in an average 97 ± 1% decrease in eYFP fluorescence for cultures with sgRNAs and dCas9 (**Figure 5E**).

Growth analyses showed that expressing dCas9 under the control of the RhaS/P_{rhaBAD}, P_{trcE*} or PhlF/P_{phlF} system with their respective inducer molecules did not impair growth

(Supplementary Figure S4B-D). Overall, our results show that the PhlF/P_{phlF} system tightly regulated dCas9 expression with no measurable leakiness, while induction with DAPG provided robust transcriptional repression. Notably, similar levels of repression were observed for all four sgRNAs for each promoter tested. This was unexpected, as previous work in Vasudevan et al. (2019) showed different levels of repression for the same four sgRNAs in PCC 6803, and may indicate that PCC 11901 is more amenable to CRISPRi repression.

We next tested the PhlF/P_{phlF} CRISPRi-dCas9 system on two endogenous gene targets in PCC 11901 to characterise its capacity for affecting native metabolism. Our gene targets were *cpcB* and *nblA*, which are involved in the synthesis and degradation of phycobiliproteins, respectively, and have been targeted previously in CRISPR-based studies in PCC 7002 and UTEX 2973 (Gordon et al., 2016; Ungerer and Pakrasi, 2016; Wendt et al., 2016). The *cpc* operon is involved in the synthesis of the phycocyanin rods of the phycobilisome complex (**Figure 5F**), an assemblage of proteins that bind to photosystem I or II and increase the efficiency of light harvesting (Puzorjov and McCormick, 2020; Domínguez-Martín et al., 2022). We designed an 18 bp sgRNA targeting *cpcB* (**Supplementary Table S3**), the first gene of the *cpc* operon, and checked to ensure that no off-target sites were present in the genome of PCC 11901 (Bae et al., 2014). Following induction with DAPG, we found that the CRISPRi strain expressing dCas9 and the sgRNA targeting *cpcB* had turned a yellow-green colour after 24 h of induction, similar to the olive colour observed in phycobilisome-deficient PCC 6803 mutants (**Figure 5G**) (Lea-Smith et al., 2014; Vasudevan et al., 2019), and its growth was reduced compared to the controls (**Figure 5H**). A significant decrease in the absorption peak at 625 nm was also observed in phycobilisome extracts from the latter strain (**Figure 5I**), demonstrating a robust reduction in phycobilisome abundance. SDS-PAGE analysis of phycobilisome extracts showed a decrease in both *cpc* and *apc* peptides in the induced (but not uninduced) CRISPRi strain, indicating that CRISPRi repression of *cpcB* resulted in a reduction in overall phycobilisome abundance in PCC 11901 (**Supplementary Figure S5A**). The apparent co-repression of allophycocyanin was unexpected, as previous *cpc* mutants in PCC 6803 showed no reduction of allophycocyanin (Lea-Smith et al., 2014; Liberton et al., 2017). However, previous attempts to knockout *cpcB* in PCC 7002 (the closest relative species to PCC 11901) failed , suggesting that *cpcB* is essential in PCC 7002 (Gordon et al., 2016). Our results indicate that phycocyanin and allophycocyanin may be co-regulated in PCC 11901, which may also be the case in PCC 7002. Measurement of

chlorophyll content in the CRISPRi strains showed no significant differences (**Supplementary Figure S5B**), suggesting that the abundance of other components of the light reactions were not affected by the repression of *cpcB*. Finally, we tested if removal of DAPG could derepress *cpcB* and restore the phycobilisome pool. Washing the cells in fresh media to remove DAPG resulted in increased growth after 24 h and restoration of phycobilisome abundance to wild-type levels after 48 h (**Supplementary Figure S5C** and **S5D**). Thus, our results indicate that ~24 h is sufficient for the turnover and degradation of the dCas9 pool in PCC 11901.

We next targeted the *nblA* gene, which plays a key role in phycobilisome degradation under nitrogen deficient conditions (**Figure 5J, Supplementary Table S3**) (Collier and Grossman, 1994). *nblA* is a common target to test CRISPR-Cas functionality in cyanobacteria as disruption of *nblA* leads to an easily detectable phenotype under nitrogen-limiting conditions; wild-type strains grown in media lacking nitrate exhibit chlorosis or bleaching characteristic of phycobilisome degradation, while *nblA* mutants show a non-bleaching phenotype and remain blue-green (Wendt et al., 2016; Baldanta et al., 2022; Cengic et al., 2022). Following induction with DAPG in nitrogen-depleted medium, we found that the CRISPRi strain expressing dCas9 and the sgRNA targeting *nblA* remained blue-green, whereas all the controls turned chlorotic (**Figure 5K**). All cultures grew very slowly due to the lack of nitrogen (**Figure 5L**), which is not unexpected as nitrogen plays a crucial role in the fast-growing phenotype of PCC 11901 (Włodarczyk et al., 2020). Chlorophyll content was reduced overall (**Supplementary Figure S5E**), indicating that all cultures were stressed. Nevertheless, a strong absorption peak at 625 nm was maintained in phycobilisome extracts from the functional CRISPRi strain, while all other controls showed a much-reduced peak indicative of phycobilisome degradation (**Figure 5M**).

Overall, the PhlF/P_{phlF} inducible CRISPRi system shows tight regulation of dCas9 activity and robust repression of heterologous and native gene expression. Furthermore, we have shown that removal of the inducer DAPG can reversibly attenuate gene repression and related physiological effects rapidly in PCC 11901. This system should provide a powerful tool for studying gene function in PCC 11901 and enable metabolic engineering approaches to exploit the yield potential of PCC 11901 (Li et al., 2016; Yao et al., 2020; Miao et al., 2023).

Markerless gene editing using CRISPR-Cas12a and a 'double HR' approach

469 The generation of markerless mutants has key advantages for biotechnology as strains can be
470 repeatedly genetically manipulated and the absence of genes encoding antibiotic resistance
471 proteins avoids the possibility of antibiotic resistant organisms being released into the
472 environment (Lea-Smith et al., 2016). However, recent efforts to use the common negative
473 selection markers *sacB* and *codA* to generate markerless mutants proved unsuccessful in PCC
474 11901 (Mills et al., 2022). To overcome this, we attempted to use a CRE-lox recombination
475 system approach recently demonstrated in PCC 7002 (Jones et al., 2021). This system first
476 involved generation of marked mutants via insertion of an AbR flanked by two LoxP sites,
477 lox71 (5'-ATAACTTCGTATAATGTATGCTATACGAACGGTA-3') and lox66 (5'-
478 TACCGTTCGTATAATGTATGCTATACGAAGTTAT-3') into a target site. A plasmid
479 vector encoding CRE and a second AbR was then introduced into marked mutants and
480 integrated into an essential locus (*rbcLXS* or *psbEFJL*) with CRE under control of the native
481 promoter. As these genes are essential, the strains were maintained in a partially segregated
482 state under antibiotic selection. Subsequent expression of CRE resulted in excision of the
483 lox71-AbR-lox66 cassette from the genome. Growth of these mutants on plates lacking the
484 second antibiotic resulted in loss of chromosomes containing the CRE/AbR insertion and
485 generation of markerless mutants. We attempted to replicate this system in PCC 11901.
486 Marked, segregated mutants targeting five different loci (*ctaDIEI*, *ctacII*, *acs*, *ldhA*, *sdhA*)
487 were successfully generated using a gentamicin resistance cassette (GmR) or KmR flanked
488 by lox66 and lox71 (**Supplementary Figure S6)**. We then generated two plasmids that
489 allowed recombination of CRE and SpR into the *rbcLXS* or *psbEFJL* locus. However, despite
490 repeated attempts to transform these plasmids into each of the five markerless mutants, we
491 were unable to obtain spectinomycin resistant colonies. Moreover, no colonies were obtained
492 when the plasmids were introduced into wild-type cells. Our inability to generate markerless
493 mutants in PCC 11901 using this approach suggests that CRE is either toxic or that the
494 generation of partially segregated mutants in key essential genes is extremely challenging.
495
496 In conjunction, alternate CRISPR-Cas gene editing approaches for generating markerless
497 mutants were trialled. These allow for more efficient engineering in cyanobacteria without
498 the requirement for positive selection markers. As the double stranded breaks generated by
499 Cas proteins are lethal to most microbes (including cyanobacteria) due to their general lack of
500 a non-homologous end joining pathway (Su et al., 2016), selection is based on the uptake of
501 supplied repair template sequences to replace the sgRNA target locus by HR (Behler et al.,
502 2018). Due to the documented cytotoxicity of Cas9 in cyanobacteria (Li et al., 2016;

503 Racharaks et al., 2021), much CRISPR-Cas work to date has focused on reportedly non-toxic
504 Cas12a (*Fn*Cpf1), which has led to several successful examples of gene editing in a variety of
505 cyanobacteria (Lin et al., 2021; Baldanta et al., 2022). Recently, an RNA riboswitch-
506 inducible dCas9 system was demonstrated in PCC 6803 that could overcome the toxicity of
507 Cas9 (Cengic et al., 2022).
508
509 Here, we sought to build a novel CyanoGate-compatible inducible CRISPR-Cas12a system
510 that allows for the generation of markerless mutants and multiplex editing at high
511 efficiencies. Our system is comprised of two vectors i) an RSF1010-based (pPMQSK1-1)
512 self-replicating 'editing vector' carrying Cas12a (pC1.509, **Supplementary Table S1**), and
513 ii) a pUC19-T 'hybrid suicide vector' designed to deliver an sgRNA expression cassette into
514 the editing vector for stable expression and a repair template with homology to the sgRNA
515 target locus on the genome by two separate HR events, which we called the 'double HR'
516 approach (**Figure 6A**). We chose the DAPG-inducible PhlF/P_{phlF} promoter system to drive
517 expression of Cas12a, which we have previously shown to be tightly regulated in PCC 11901
518 (**Figure 4** and **Figure 5**), and conjugated the editing vector into PCC 11901 to generate an
519 'editing strain'. To assist with assembling the hybrid suicide vector, we constructed the
520 CyanoGate-compatible sgRNA assembly acceptor vector pCA0.421 based on the CRATES
521 system from Liao et al., (2019), which enables one-pot assembly of single or multiplexed
522 sgRNA arrays for targeted gene editing (**Supplementary Table S1**). We hypothesised that
523 with this approach new hybrid suicide vectors carrying one or more sgRNAs and up to six
524 repair templates could be rapidly generated and iteratively transformed into the editing strain
525 to generate markerless mutants with single or multiple chromosomal alterations.
526
527 As a proof-of-concept, we used the editing strain (carrying the editing vector with SpR) to
528 perform a markerless knock-in of an eYFP expression cassette into the *mrr* neutral site
529 (**Figure 6B**). A hybrid suicide vector pCT.590 (**Supplementary Table S2**) was assembled
530 and transformed into PCC 11901 in the absence or presence of DAPG, and the transformation
531 mix was then plated onto gentamicin-supplemented agar or gentamicin- and DAPG-
532 supplemented agar, respectively. In the absence of DAPG, no edits were observed in the
533 colonies that grew, indicating that Cas12a expression was tightly repressed. However, with
534 DAPG we observed that 25% of colonies showed insertions of the eYFP expression cassette
535 and eYFP fluorescence. This demonstrated that in the Δ*mrr*::eYFP colonies i) HR had
536 occurred between the hybrid vector and the editing vector to allow for growth on gentamicin,

537 and ii) HR had occurred between the hybrid vector and the genome. In the remaining 75% of
538 colonies, only i) had occurred, which indicated that HR with the editing vector was more
539 prominent than with the genome. We confirmed that double HR had occurred with colonies
540 expressing eYFP by PCR of the editing vector, which showed the presence of the sgRNA
541 cassette and that SpR had been replaced by GmR (**Supplementary Figure S9**). Notably, the
542 absence of a WT band in the Δ*mrr*::eYFP colonies indicated that these strains were fully
543 segregated.
544
545 To further improve the efficiency of editing, we performed transformation in the absence of
546 DAPG for 4 h, then added DAPG for 12 h before plating onto gentamicin- and DAPG-
547 supplemented agar to induce Cas12a expression. We observed a significant increase in the
548 efficiency of double HR (81%) (**Figure 6B**), which demonstrated the benefit of increasing the
549 time period for genomic HR to occur prior to the induction of Cas12a expression. This
550 approach was used in all subsequent gene editing experiments. We next assembled the hybrid
551 suicide vector pCT.621 to test the *aquI* neutral site as a second target locus for insertion of an
552 mCherry expression cassette (**Supplementary Table S2**). Here we observed a 56%
553 efficiency in generating fully segregated Δ*aquI*::mCherry lines (**Figure 6C**), suggesting that
554 the double HR approach was still robust at different genomic loci.
555
556 We next investigated if we could generate the double insertion mutant Δ*mrr*::eYFP/
557 Δ*aquI*::mCherry through iterative or multiplex genome editing. For the former, we assembled
558 a hybrid suicide vector pCT.622 for transformation into Δ*mrr*::eYFP, which carries an editing
559 vector with GmR (**Supplementary Table S2**). Following transformation of Δ*mrr*::eYFP, we
560 observed mCherry expression cassette insertions in *aquI* in 31% of colonies (**Figure 6D**).
561 Fluorescence measurements confirmed expression of both eYFP and mCherry, and thus
562 successful generation of Δ*mrr*::eYFP/ Δ*aquI*::mCherry double mutants through iterative gene
563 editing. For the latter multiplex approach, we assembled the suicide vector pCT.623 carrying
564 an sgRNA array and homology repair templates designed to insert expression cassettes for
565 eYFP and mCherry into *mrr* and *aquI*, respectively. Following transformation of the editing
566 strain, we screened colonies for single and double insertion mutants by PCR. We observed
567 insertion efficiencies of 56% and 25% for the eYFP and mCherry expression cassettes,
568 respectively, while 25% of the colonies contained both cassettes at their expected loci
569 (**Figure 6E**). Notably, we did not find examples of an mCherry insertion in the absence of

eYFP, suggesting that the first sgRNA in the array targeting the *mrr* locus may have been more efficient or is more abundantly expressed.

Overall, our results support PCC 11901 as a highly amenable strain for CRISPR-Cas12a-based editing. To our knowledge, this is the first report of iterative CRISPR-Cas12a gene editing and multiplex editing using an sgRNA array in a cyanobacterial strain. The iterative editing scheme was designed to allow as many sites to be targeted as desired, by cycling through SpR and GmR cassettes in the hybrid suicide vector, enabling more complex editing schemes to occur. The two editing schemes (iterative and multiplex) could also be further combined, allowing further flexibility in strain design. Additional efficiency improvements could be made by establishing the mechanism by which 'escaper colonies' survive on selective media but avoid editing, a common phenomenon observed in bacteria and cyanobacteria (Vento et al., 2019; Cengic et al., 2022). As we were able to achieve iterative gene editing, escape was not due to mutations in Cas12a and thus may have been due to point mutations in the sgRNA or the sgRNA genomic target site. A possible strategy to improve the efficiency of edits could be to reduce the expression levels of Cas12a and/or the sgRNA(s), an approach that that has been shown to increase editing efficiencies in *E. coli* and *Klebsiella* spp. (Collias et al., 2023).

Finally, we sought to cure the editing strain of the self-replicating editing vector. Various methods have been employed to cure plasmids from bacteria, with the standard approach being repeated subculture of mutants in antibiotic-free medium and screening for spontaneous plasmid loss (Bishé et al., 2019). However, RSF1010-based vectors appear to persist in cyanobacteria for long periods, even in the absence of antibiotic selection (Nagy et al., 2021; Puzorjov et al., 2022). Previous CRISPR-Cas work in *E. coli* and *P. putida* utilised a 'self-targeting' sgRNA for efficient removal of RSF1010-based vectors (Lauritsen et al., 2017). Here, we generated a hybrid suicide vector containing an sgRNA that targeted the editing vector pC1.509. We transformed cells in the presence of DAPG and plated the transformation culture onto agar without antibiotics. We then screened colonies for the absence of the editing vector by PCR and observed a curing efficiency of 50% (**Figure 6F**). We further verified the loss of the editing vector by patching the cured colonies onto gentamicin-supplemented agar, which resulted in no growth indicating sensitivity to the antibiotic. Thus, we demonstrated that PCC 11901 mutants generated by CRISPR-Cas12a

603 can be cured of the editing vector to produce fully markerless mutant strains containing no
604 scars or AbR cassettes.
605
606 **CONCLUSION**
607 Here we have investigated the amenability of the fast-growing marine cyanobacterium PCC
608 11901 to engineering and assembled a comprehensive suite of tools compatible with the
609 CyanoGate MoClo platform to enable future work in this strain. We hope that the tools
610 described will accelerate the wider adoption of this next-generation cyanobacterial chassis
611 strain. The fast-growing and highly productive phenotype of PCC 11901 offers much in terms
612 of advancing our fundamental understanding of the genetic basis and regulation of these
613 processes (Ungerer et al., 2018). Furthermore, PCC 11901 shows promise for applied work
614 aiming to develop commercially viable green biotechnology chassis for renewable
615 biomanufacture and biomaterials production (Goodchild-Michelman et al., 2023),
616 sequestration of CO_2 emissions in hard-to-abate sectors (e.g. capture of CO_2 from point-
617 source flue gases) (Zhang et al., 2017), and sustainable space exploration (Santomartino et
618 al., 2023).
619
620 **MATERIALS AND METHODS**
621 **Cyanobacterial culture conditions**
622 *Synechococcus* sp. PCC 11901 was cultured in AD7 or MAD liquid medium (Włodarczyk et
623 al., 2020), or on 1.5% (w/v) agar plates as described in (Włodarczyk et al., 2020). Cultures
624 were grown in an Algaetron AG 230 incubator (Photon Systems Instruments) at 30°C, 2%
625 (v/v) CO_2 under continuous warm white LED light (150 µmol photons m^{-2} s^{-1}) and shaking at
626 120 rpm. Agar plates were incubated under identical conditions, without shaking.
627
628 **Plasmid vector assembly**
629 Level 0, 1, and T plasmid vectors were assembled using the CyanoGate MoClo kit
630 (Vasudevan et al., 2019). Native PCC 11901 genetic parts were amplified from genomic
631 DNA using Q5 High-Fidelity DNA Polymerase (New England Biolabs). Where necessary,
632 native genetic parts were domesticated (i.e. sites for Type IIS restriction endonucleases BsaI
633 and BpiI were removed) using specific primers. Alternatively, parts were synthesized as
634 Gblocks DNA fragments (Integrated DNA Technologies) and cloned directly into an
635 appropriate level 0 acceptor (Engler et al., 2014) (see **Supplementary Table S1** and
636 **Supplementary Data S1** for new vectors, and **Supplementary Table S2** for all plasmids

assembled in this study). Vectors were transformed into One Shot TOP10 chemically competent *Escherichia coli* (Thermo Fisher Scientific) cells as per the manufacturer's instructions. Transformed cultures were grown at 37°C on 1.5% (w/v) LB agar or in liquid LB medium shaking at 125 rpm with appropriate antibiotic selection.

sgRNA selection and CRISPR-Cas assemblies

sgRNAs were designed by selecting 18-22 bp sequences adjacent to the protospacer adjacent motif (PAM) sequence 5'-NGG-3' for *Streptococcus pyogenes* dCas9 or 5'-TTTV-3' for *Francisella novicida* Cas12a. Candidate sgRNAs were checked for potential off-target sites in the PCC 11901 genome using Cas-OFFinder (Bae et al., 2014). The sgRNAs for dCas9 were made by annealing complementary oligonucleotides carrying the required overhangs and BsaI recognition sites (**Supplementary Table S3**), and were assembled into the level 1 position 2 (L1P2) acceptor vector pICH47742 together with the P_{trc10_TSS} promoter (pC0.220) and the sgRNA scaffold (pC0.122) as described in Vasudevan et al., (2019). The sgRNAs for Cas12a were also made by annealing complementary oligonucleotides carrying overhangs and BpiI recognition sites as described in Liao et al. (2019) (see **Supplementary Figure S3** and **S7**) and were assembled into the new acceptor vector pC0.421 (**Supplementary Table S1**).

Natural transformation of PCC 11901

Purified plasmid (1 µg) was added to 1 mL of wild-type PCC 11901 culture at exponential growth phase (OD_{750} = 0.8) and incubated for 12 h at 30°C under continuous warm white LED light (150 µmol photons m^{-2} s^{-1}) and shaking at 120 rpm in an Infors Multitron Pro incubator (Infors HT). The cultures were then plated onto AD7 agar plates supplemented with appropriate antibiotics (25 µg mL^{-1} spectinomycin, 50 µg mL^{-1} gentamicin, 100 µg mL^{-1} carbenicillin or 100 µg mL^{-1} kanamycin). Plates were then sealed with 3M Micropore® tape to allow for gas exchange and incubated at 30°C, 2% (v/v) CO_2 under warm white LED light (150 µmol photons m^{-2} s^{-1}). Colonies typically appeared after 2-4 days.

Transconjugation of PCC 11901

Genetic modification by conjugal transfer was performed using an approach adapted from Gale et al. (2019). Overnight cultures of *E. coli* strain HB101 harbouring vectors pRK2013 (ATCC 37159) and pRL528 (the helper strain) and a TOP10 strain harbouring an RSF1010-derived level T vector were each washed three times with LB medium to remove antibiotics.

671 The *E. coli* cultures were then combined (450 µL each) and incubated for 1 h at room
672 temperature (RT). PCC 11901 cultures were grown to OD_{750} ~1.0 and washed three times
673 with fresh AD7 medium. The combined *E. coli* culture was added to 900 µL of PCC 11901
674 culture and the mixture incubated at 30°C under warm white LED light (150 µmol photons
675 m^{-2} s^{-1}) for 4 h, without shaking. The mix was centrifuged at 4,000 *g* and the cell pellet was
676 plated onto 0.45 µm Metricel® membrane filter discs (Pall Corporation) laid on top of non-
677 selective AD7 agar. After 24 h of incubation, the membranes were transferred to AD7 agar
678 supplemented with appropriate antibiotics (25 µg mL^{-1} spectinomycin, or 100 µg mL^{-1}
679 kanamycin) and incubated as above. Conjugant colonies typically appeared six days post
680 membrane transfer.
681
682 **Comparative growth assays**
683 Growth curve experiments were performed by inoculating a seed culture containing 30 mL of
684 MAD medium with single colonies of cyanobacteria picked from agar plates and grown as
685 described above to OD_{750} ~1.0. The seed cultures were then used to prepare triplicate 15 mL
686 starter cultures adjusted to OD_{750} ~0.2 and aliquoted into Corning® 25 cm^2 cell culture flasks
687 with canted necks and vented caps (Corning). To facilitate gas exchange and prevent
688 foaming, 0.5 µL of Antifoam 204 (Sigma Aldrich) was added to the cultures. Cultures were
689 grown at 30°C, 2% (v/v) CO_2, shaking at 150 rpm under 150 µmol photons m^{-2} s^{-1} for the
690 first 24 h, which was then increased to 750 µmol photons m^{-2} s^{-1}. Optical density was
691 measured every 24 h using a WPA Biowave II UV-Vis spectrophotometer (Biochrom) for
692 eight days.
693
694 **eYFP quantifications**
695 Mutant PCC 11901 strains were grown in 6-well culture plates (Starlab CytoOne) and
696 incubated in an Algaetron® AG 230 incubator under the same culturing conditions as
697 described above. OD_{750} and eYFP fluorescence of cultures were measured using a FLUOstar
698 OMEGA microplate reader (BMG Labtech). Fluorescence of eYFP for individual cells
699 (10,000 cells per culture) was measured by flow cytometry using a BD® LSR II Fortessa
700 flow cytometer (Becton Dickinson). Cells were gated using forward and side scatter, and
701 median eYFP fluorescence was calculated from excitation/emission wavelengths 488
702 nm/515–545 nm (Kelly et al., 2018), and reported after 24 h of growth unless otherwise
703 stated.
704

705 **Terminator efficiency calculations**

706 The efficiency of terminator sequences (terminator efficiency (TE)) was calculated by
707 assembling terminator sequences into the pDUOTK1-L1 vector as described in Gale et al.,
708 (2021).

709

710 **Measurement of chlorophyll content**

711 Cultures were diluted to OD_{750} = 1.0 and centrifuged at 17,000 *g* for 2 min. The resulting
712 pellet was resuspended in 100% (v/v) methanol and shaken at 2400 rpm for 1 h in the dark at
713 RT using an IKA-VIBRAX-VXR bead beater. The homogenates were then centrifuged at
714 17,000 *g* for 10 min and the absorbance of the supernatant was measured at 652, 665 and
715 750 nm. The mean concentration of chlorophyll *a* was calculated from triplicates as described
716 in Porra et al., (1989).

717

718 **Extraction of phycobiliproteins and analysis**

719 Phycobiliproteins (PBS) were extracted and quantified using absorbance spectroscopy as
720 described previously (Zavřel et al., 2018). Briefly, PCC 11901 cells were pelleted by
721 centrifugation at 15,000 *g* for 5 min, washed in phosphate buffered saline three times and
722 freeze-dried overnight. Dried samples were lysed with 0.5 mm glass beads (BioSpec
723 Products) on a TissueLyser II homogeniser (Qiagen) for 15 s at RT. 1 mL of pre-cooled
724 phosphate buffered saline at 4°C was added to each tube and mixed for 5 s on the
725 homogeniser. Samples were then incubated on ice for 60 min to efficiently extract soluble
726 proteins and prevent protein degradation. Following centrifugation for 5 min at 4°C and
727 15,000 *g*, the aqueous blue liquid layer containing PBS was transferred to sterile 1.5 mL
728 microcentrifuge tubes and frozen for future use. Samples were measured from 550-750 nm on
729 a Biochrom WPA Biowave II Spectrophotometer. For SDS-PAGE analysis, samples were
730 run on a Bolt 12% Bis-Tris Plus Mini protein gel (Invitrogen) at 150 V for 1 h. A pre-stained
731 protein standard (Proteintech) was used as a ladder. The gels were then stained with 1% (w/v)
732 Coomassie Brilliant Blue solution (Bio-Rad) and destained with a methanol: acetic acid:
733 distilled water (50%: 10%: 40%) solution.

734

735 **ACKNOWLEDGEMENT**

736 We would like to thank the Frankenberg-Dinkel Lab (RPTU Kaiserslautern-Landau) for
737 kindly providing their facilities for several experiments while hosting A.J.V.

738

DATA AVAILABILITY

Plasmids in **Supplementary Table S1** are available from Addgene (https://www.addgene.org/Alistair_McCormick), Addgene IDs: 203934-203943, 205441.

FUNDING

A.J.V. was funded by a postgraduate research scholarship from the Darwin Trust of Edinburgh. T.T.S. acknowledges funding from the Green Chemicals Beacon of Excellence, University of Nottingham. J.A.M.C. acknowledges funding support from a FEBS short term fellowship and University of Cordoba fellowship. L.A.M. acknowledges funding support from the BBSRC Norwich Research Park Doctoral Training Partnership program (grant number BB/S507404/1). D.J. and L.-S. acknowledge funding from BBSRC grant [BB/S020365/1]. A.J.M acknowledges funding from the UK Biotechnology and Biological Sciences Research Council (BBSRC) grants [BB/S020128/1] and [BB/W003538/1].

COMPETING INTERESTS

The authors declare that no competing interests exist.

SUPPLEMENTARY DATA

Supplementary Table S1. Table of all new CyanoGate-compatible parts generated in this work.

Supplementary Table S2. All plasmids made and used in this study. See 'Supplementary Table S2 - Plasmids (all).xlsx'.

Supplementary Table S3. Primer and sgRNA oligonucleotides used in this study. See 'Supplementary Table S3 - Primer and sgRNA oligonucleotides.xlsx'.

Supplementary Data S1. Sequence maps (.gb files) for plasmid vectors in Supplementary Table S1. See 'Supplementary Data S1.zip'.

Supplementary Figure S1. Analysis of putative Gcn5-related N-acetyltransferase (GNAT) family genes in PCC 11901.

Supplementary Figure S2. Representative PCR-based segregation analysis of PCC 11901 transformants targeting neutral sites *glgA1* and *aquI*.

Supplementary Figure S3. Growth of PCC 11901 with varying doses of small molecule inducers.

Supplementary Figure S4. Growth analysis of CRISPRi-dCas9 strains targeting eYFP.

Supplementary Figure S5. Analysis of CRISPRi-dCAs9 strains targeting *cpcB* and *nblA*.

773 **Supplementary Figure S6.** Attempted generation of markerless mutants using the CRE-Lox
774 system.
775 **Supplementary Figure S7**. CRISPR-Cas12a double HR editing approach – sgRNA, repair
776 template and hybrid suicide vector assembly.
777 **Supplementary Figure S8**. Pipeline for iterative CRISPR-Cas12a editing using the double
778 HR approach.
779 **Supplementary Figure S9.** Confirmation of recombination between the hybrid suicide
780 vector and editing vector.
781

782 **REFERENCES**

783 **Abbas A, Morrissey JP, Marquez PC, Sheehan MM, Delany IR, O'Gara F** (2002)
784 Characterization of interactions between the transcriptional repressor PhlF and its
785 binding site at the phlA promoter in Pseudomonas fluorescens F113. J Bacteriol **184**:
786 3008–3016
787 **Bae S, Park J, Kim J-S** (2014) Cas-OFFinder: a fast and versatile algorithm that searches
788 for potential off-target sites of Cas9 RNA-guided endonucleases. Bioinformatics **30**:
789 1473–1475
790 **Baldanta S, Guevara G, Navarro-Llorens JM** (2022) SEVA-Cpf1, a CRISPR-Cas12a
791 vector for genome editing in cyanobacteria. Microb Cell Factories **21**: 103
792 **Batterton JC, Van Baalen C** (1971) Growth responses of blue-green algae to sodium
793 chloride concentration. Archiv Mikrobiol **76**: 151–165
794 **Behle A, Saake P, Germann AT, Dienst D, Axmann IM** (2020) Comparative dose–
795 response analysis of inducible promoters in cyanobacteria. ACS Synth Biol **9**: 843–855
796 **Behler J, Vijay D, Hess WR, Akhtar MK** (2018) CRISPR-based technologies for metabolic
797 engineering in cyanobacteria. Trends Biotechnol **36**: 996–1010
798 **BEIS** (2021) 'Net Zero Strategy: Build Back Greener'. Department for Business, Energy, and
799 International Strategy. Available at: https://www.gov.uk/government/publications/net-
800 zero-strategy (Accessed: 13 September 2022).
801 **Bernhards CB, Liem AT, Berk KL, Roth PA, Gibbons HS, Lux MW** (2022) Putative
802 phenotypically neutral genomic insertion points in prokaryotes. ACS Synth Biol **11**:
803 1681–1685
804 **Bishé B, Taton A, Golden JW** (2019) Modification of RSF1010-based broad-host-range
805 plasmids for improved conjugation and cyanobacterial bioprospecting. iScience **20**:
806 216–228
807 **Cameron JC, Pakrasi HB** (2011) Glutathione facilitates antibiotic resistance and
808 photosystem I stability during exposure to gentamicin in cyanobacteria. Appl Environ
809 Microbiol **77**: 3547–3550
810 **Cengic I, Cañadas IC, Minton NP, Hudson EP** (2022) Inducible CRISPR/Cas9 allows for
811 multiplexed and rapidly segregated single-target genome editing in Synechocystis sp.
812 PCC 6803. ACS Synth Biol **11**: 3100–3113
813 **Chen Y-J, Liu P, Nielsen AAK, Brophy JAN, Clancy K, Peterson T, Voigt CA** (2013)
814 Characterization of 582 natural and synthetic terminators and quantification of their
815 design constraints. Nat Methods **10**: 659–664

Chi X, Zhang S, Sun H, Duan Y, Qiao C, Luan G, Lu X (2019) Adopting a theophylline-responsive riboswitch for flexible regulation and understanding of glycogen metabolism in synechococcus elongatus PCC 7942. Front Microbiol 10:

Cho BA, Moreno-Cabezuelo JÁ, Mills LA, del Río Chanona EA, Lea-Smith DJ, Zhang D (2023) Integrated experimental and photo-mechanistic modelling of biomass and optical density production of fast versus slow growing model cyanobacteria. Algal Res **70**: 102997

Collias D, Vialetto E, Yu J, Co K, Almási É d H, Rüttiger A-S, Achmedov T, Strowig T, Beisel CL (2023) Systematically attenuating DNA targeting enables CRISPR-driven editing in bacteria. Nat Commun **14**: 680

Collier JL, Grossman AR (1994) A small polypeptide triggers complete degradation of light-harvesting phycobiliproteins in nutrient-deprived cyanobacteria. EMBO J **13**: 1039–1047

Dallo T, Krishnakumar R, Kolker SD, Ruffing AM (2023) High-Density Guide RNA Tiling and Machine Learning for Designing CRISPR Interference in Synechococcus sp. PCC 7002. ACS Synth Biol. doi: 10.1021/acssynbio.2c00653

Daneshvar E, Wicker RJ, Show P-L, Bhatnagar A (2022) Biologically-mediated carbon capture and utilization by microalgae towards sustainable CO2 biofixation and biomass valorization – A review. Chem Eng J **427**: 130884

Depardieu F, Bikard D (2020) Gene silencing with CRISPRi in bacteria and optimization of dCas9 expression levels. Methods **172**: 61–75

Dias E, Oliveira M, Jones-Dias D, Vasconcelos V, Ferreira E, Manageiro V, Caniça M (2015) Assessing the antibiotic susceptibility of freshwater Cyanobacteria spp. Front Microbiol **6**: 799

Domínguez-Martín MA, Sauer PV, Kirst H, Sutter M, Bína D, Greber BJ, Nogales E, Polívka T, Kerfeld CA (2022) Structures of a phycobilisome in light-harvesting and photoprotected states. Nature **609**: 835–845

Engler C, Youles M, Gruetzner R, Ehnert T-M, Werner S, Jones JDG, Patron NJ, Marillonnet S (2014) A golden gate modular cloning toolbox for plants. ACS Synth Biol **3**: 839–843

Favrot L, Blanchard JS, Vergnolle O (2016) Bacterial GCN5-Related N-Acetyltransferases: From Resistance to Regulation. Biochemistry **55**: 989–1002

Fontana J, Dong C, Ham JY, Zalatan JG, Carothers JM (2018) Regulated expression of sgRNAs tunes CRISPRi in E. coli. Biotechnology Journal **13**: 1800069

Gale GAR, Schiavon Osorio AA, Mills LA, Wang B, Lea-Smith DJ, McCormick AJ (2019) Emerging species and genome editing tools: future prospects in cyanobacterial synthetic biology. Microorganisms **7**: 409

Gale GAR, Wang B, McCormick AJ (2021) Evaluation and comparison of the efficiency of transcription terminators in different cyanobacterial species. Front Microbiol 11:

Goodchild-Michelman IM, Church GM, Schubert MG, Tang T-C (2023) Light and carbon: Synthetic biology toward new cyanobacteria-based living biomaterials. Mater Today Bio **19**: 100583

Gordon GC, Korosh TC, Cameron JC, Markley AL, Begemann MB, Pfleger BF (2016) CRISPR interference as a titratable, trans-acting regulatory tool for metabolic engineering in the cyanobacterium Synechococcus sp. strain PCC 7002. Metab Eng **38**: 170–179

Hitchcock A, Hunter CN, Canniffe DP (2020) Progress and challenges in engineering cyanobacteria as chassis for light-driven biotechnology. Microb Biotechnol **13**: 363–367

Huang H-H, Lindblad P (2013) Wide-dynamic-range promoters engineered for cyanobacteria. J Biol Eng **7**: 10

866 **Iwai M, Katoh H, Katayama M, Ikeuchi M** (2004) Improved genetic transformation of the
867 thermophilic cyanobacterium, thermosynechococcus elongatus BP-1. Plant Cell Physiol
868 **45**: 171–175
869 **Jaiswal D, Sengupta A, Sengupta S, Madhu S, Pakrasi HB, Wangikar PP** (2020) A novel
870 cyanobacterium Synechococcus elongatus PCC11802 has distinct genomic and
871 metabolomic characteristics compared to its neighbor PCC 11801. Sci Rep **10**: 191
872 **Jaiswal D, Sengupta A, Sohoni S, Sengupta S, Phadnavis AG, Pakrasi HB, Wangikar**
873 **PP** (2018) Genome features and biochemical characteristics of a robust, fast growing
874 and naturally transformable cyanobacterium Synechococcus elongatus PCC11801
875 isolated from India. Sci Rep **8**: 16632
876 **Jester BW, Zhao H, Gewe M, Adame T, Perruzza L, Bolick DT, Agosti J, Khuong N,**
877 **Kuestner R, Gamble C, et al** (2022) Development of spirulina for the manufacture and
878 oral delivery of protein therapeutics. Nat Biotechnol **40**: 956–964
879 **Jones CM, Parrish S, Nielsen DR** (2021) Exploiting polyploidy for markerless and plasmid-
880 free genome engineering in cyanobacteria. ACS Synth Biol **10**: 2371–2382
881 **Kavita K, Breaker RR** (2023) Discovering riboswitches: the past and the future. Trends
882 Biochem Sci **48**: 119–141
883 **Kelly CL, Taylor GM, Hitchcock A, Torres-Méndez A, Heap JT** (2018) A rhamnose-
884 inducible system for precise and temporal control of gene expression in cyanobacteria.
885 ACS Synth Biol **7**: 1056–1066
886 **Khetkorn W, Incharoensakdi A, Lindblad P, Jantaro S** (2016) Enhancement of poly-3-
887 hydroxybutyrate production in Synechocystis sp. PCC 6803 by overexpression of its
888 native biosynthetic genes. Bioresour Technol **214**: 761–768
889 **Kopka J, Schmidt S, Dethloff F, Pade N, Berendt S, Schottkowski M, Martin N,**
890 **Dühring U, Kuchmina E, Enke H, et al** (2017) Systems analysis of ethanol production
891 in the genetically engineered cyanobacterium Synechococcus sp. PCC 7002. Biotechnol
892 Biofuels **10**: 56
893 **Kufryk GI, Sachet M, Schmetterer G, Vermaas WFJ** (2002) Transformation of the
894 cyanobacterium Synechocystis sp. PCC 6803 as a tool for genetic mapping: optimization
895 of efficiency. FEMS Microbiol Lett **206**: 215–219
896 **Lauritsen I, Porse A, Sommer MOA, Nørholm MHH** (2017) A versatile one-step
897 CRISPR-Cas9 based approach to plasmid-curing. Microb Cell Factories **16**: 135
898 **Lea-Smith DJ, Bombelli P, Dennis JS, Scott SA, Smith AG, Howe CJ** (2014)
899 Phycobilisome-deficient strains of Synechocystis sp. PCC 6803 have reduced size and
900 require carbon-limiting conditions to exhibit enhanced productivity. Plant Physiol **165**:
901 705–714
902 **Lea-Smith DJ, Summerfield TC, Ducat DC, Lu X, McCormick AJ, Purton S** (2021)
903 Editorial: Exploring the growing role of cyanobacteria in industrial biotechnology and
904 sustainability. Front Microbiol 12:
905 **Lea-Smith DJ, Vasudevan R, Howe CJ** (2016) Generation of marked and markerless
906 mutants in model cyanobacterial species. J Vis Exp 54001
907 **Li H, Shen CR, Huang C-H, Sung L-Y, Wu M-Y, Hu Y-C** (2016) CRISPR-Cas9 for the
908 genome engineering of cyanobacteria and succinate production. Metab Eng **38**: 293–302
909 **Li S, Sun T, Xu C, Chen L, Zhang W** (2018) Development and optimization of genetic
910 toolboxes for a fast-growing cyanobacterium Synechococcus elongatus UTEX 2973.
911 Metab Eng **48**: 163–174
912 **Liberton M, Chrisler WB, Nicora CD, Moore RJ, Smith RD, Koppenaal DW, Pakrasi**
913 **HB, Jacobs JM** (2017) Phycobilisome truncation causes widespread proteome changes
914 in Synechocystis sp. PCC 6803. PLoS One **12**: e0173251

Lin P-C, Zhang F, Pakrasi HB (2021) Enhanced limonene production in a fast-growing cyanobacterium through combinatorial metabolic engineering. Metab Eng Commun **12**: e00164

Lindberg P, Park S, Melis A (2010) Engineering a platform for photosynthetic isoprene production in cyanobacteria, using Synechocystis as the model organism. Metab Eng **12**: 70–79

Liu D, Johnson VM, Pakrasi HB (2020) A reversibly induced CRISPRi system targeting photosystem II in the cyanobacterium Synechocystis sp. PCC 6803. ACS Synth Biol **9**: 1441–1449

Liu D, Pakrasi HB (2018) Exploring native genetic elements as plug-in tools for synthetic biology in the cyanobacterium Synechocystis sp. PCC 6803. Microb Cell Factories **17**: 48

Ma AT, Schmidt CM, Golden JW (2014) Regulation of gene expression in diverse cyanobacterial species by using theophylline-responsive riboswitches. Appl Environ Microbiol **80**: 6704–6713

Meyer AJ, Segall-Shapiro TH, Glassey E, Zhang J, Voigt CA (2019) Escherichia coli "Marionette" strains with 12 highly optimized small-molecule sensors. Nat Chem Biol **15**: 196–204

Meyer R (2009) Replication and conjugative mobilization of broad host-range IncQ plasmids. Plasmid **62**: 57–70

Miao R, Jahn M, Shabestary K, Hudson EP (2023) CRISPR interference screens reveal tradeoffs between growth rate and robustness in Synechocystis sp. PCC 6803 across trophic conditions. 2023.02.13.528328

Mills LA, Moreno-Cabezuelo JÁ, Włodarczyk A, Victoria AJ, Mejías R, Nenninger A, Moxon S, Bombelli P, Selão TT, McCormick AJ, et al (2022) Development of a biotechnology platform for the fast-growing cyanobacterium Synechococcus sp. PCC 11901. Biomolecules **12**: 872

Mittermair S, Lakatos G, Nicoletti C, Ranglová K, Manoel JC, Grivalský T, Kozhan DM, Masojídek J, Richter J (2021) Impact of glgA1, glgA2 or glgC overexpression on growth and glycogen production in Synechocystis sp. PCC 6803. J Biotechnol **340**: 47–56

Nakahira Y, Ogawa A, Asano H, Oyama T, Tozawa Y (2013) Theophylline-dependent riboswitch as a novel genetic tool for strict regulation of protein expression in cyanobacterium synechococcus elongatus PCC 7942. Plant Cell Physiol **54**: 1724–1735

Ng AH, Berla BM, Pakrasi HB (2015) Fine-tuning of photoautotrophic protein production by combining promoters and neutral sites in the cyanobacterium Synechocystis sp. strain PCC 6803. Appl Environ Microbiol **81**: 6857–6863

Opel F, Siebert NA, Klatt S, Tüllinghoff A, Hantke JG, Toepel J, Bühler B, Nürnberg DJ, Klähn S (2022) Generation of synthetic shuttle vectors enabling modular genetic engineering of cyanobacteria. ACS Synth Biol **11**: 1758–1771

Pinto F, Pacheco CC, Oliveira P, Montagud A, Landels A, Couto N, Wright PC, Urchueguía JF, Tamagnini P (2015) Improving a Synechocystis-based photoautotrophic chassis through systematic genome mapping and validation of neutral sites. DNA Res **22**: 425–437

Porra RJ, Thompson WA, Kriedemann PE (1989) Determination of accurate extinction coefficients and simultaneous equations for assaying chlorophylls a and b extracted with four different solvents: verification of the concentration of chlorophyll standards by atomic absorption spectroscopy. Biochim Biophys Acta - Bioenerg **975**: 384–394

Puzorjov A, Dunn KE, McCormick AJ (2021) Production of thermostable phycocyanin in a mesophilic cyanobacterium. Metab Eng Commun **13**: e00175

965 **Puzorjov A, McCormick AJ** (2020) Phycobiliproteins from extreme environments and their
966 potential applications. J Exp Bot **71**: 3827–3842
967 **Puzorjov A, Mert Unal S, Wear MA, McCormick AJ** (2022) Pilot scale production,
968 extraction and purification of a thermostable phycocyanin from Synechocystis sp. PCC
969 6803. Bioresour Technol **345**: 126459
970 **Racharaks R, Arnold W, Peccia J** (2021) Development of CRISPR-Cas9 knock-in tools for
971 free fatty acid production using the fast-growing cyanobacterial strain Synechococcus
972 elongatus UTEX 2973. J Microbiol Methods **189**: 106315
973 **Rautela A, Kumar S** (2022) Engineering plant family TPS into cyanobacterial host for
974 terpenoids production. Plant Cell Rep **41**: 1791–1803
975 **Ruffing AM, Jensen TJ, Strickland LM** (2016) Genetic tools for advancement of
976 Synechococcus sp. PCC 7002 as a cyanobacterial chassis. Microb Cell Factories **15**: 190
977 **Sakamoto T, Shen G, Higashi S, Murata N, Bryant DA** (1997) Alteration of low-
978 temperature susceptibility of the cyanobacterium Synechococcus sp. PCC 7002 by
979 genetic manipulation of membrane lipid unsaturation. Arch Microbiol **169**: 20–28
980 **Sakurai I, Stazic D, Eisenhut M, Vuorio E, Steglich C, Hess WR, Aro E-M** (2012)
981 Positive regulation of psbA gene expression by cis-encoded antisense RNAs in
982 Synechocystis sp. PCC 6803. Plant Physiol **160**: 1000–1010
983 **Santomartino R, Averesch NJH, Bhuiyan M, Cockell CS, Colangelo J, Gumulya Y,**
984 **Lehner B, Lopez-Ayala I, McMahon S, Mohanty A, et al** (2023) Toward sustainable
985 space exploration: a roadmap for harnessing the power of microorganisms. Nat Commun
986 **14**: 1391
987 **Saveria T, Parthiban C, Seilie AM, Brady C, Martinez A, Manocha R, Afreen E, Zhao**
988 **H, Krzeszowski A, Ferrara J, et al** (2022) Needle-free, spirulina-produced
989 Plasmodium falciparum circumsporozoite vaccination provides sterile protection against
990 pre-erythrocytic malaria in mice. NPJ Vaccines **7**: 1–11
991 **Selão TT** (2022) Exploring cyanobacterial diversity for sustainable biotechnology. J Exp Bot
992 **73**: 3057–3071
993 **Sengupta A, Pritam P, Jaiswal D, Bandyopadhyay A, Pakrasi HB, Wangikar PP** (2020a)
994 Photosynthetic co-production of succinate and ethylene in a fast-growing
995 cyanobacterium, Synechococcus elongatus PCC 11801. Metabolites **10**: 250
996 **Sengupta S, Jaiswal D, Sengupta A, Shah S, Gadagkar S, Wangikar PP** (2020b)
997 Metabolic engineering of a fast-growing cyanobacterium Synechococcus elongatus PCC
998 11801 for photoautotrophic production of succinic acid. Biotechnol Biofuels **13**: 89
999 **Shiraishi H, Nishida H** (2022) Complete genome sequence of the edible filamentous
1000 cyanobacterium arthrospira platensis nies-39, based on long-read sequencing. Microbiol
1001 Resour Announc **12**: e01139-22
1002 **Soini J, Ukkonen K, Neubauer P** (2008) High cell density media for Escherichia coli are
1003 generally designed for aerobic cultivations – consequences for large-scale bioprocesses
1004 and shake flask cultures. Microb Cell Factories **7**: 26
1005 **Su T, Liu F, Gu P, Jin H, Chang Y, Wang Q, Liang Q, Qi Q** (2016) A CRISPR-Cas9
1006 assisted non-homologous end-joining strategy for one-step engineering of bacterial
1007 genome. Sci Rep **6**: 37895
1008 **Taton A, Ma AT, Ota M, Golden SS, Golden JW** (2017) NOT gate genetic circuits to
1009 control gene expression in cyanobacteria. ACS Synth Biol **6**: 2175–2182
1010 **Taton A, Unglaub F, Wright NE, Zeng WY, Paz-Yepes J, Brahamsha B, Palenik B,**
1011 **Peterson TC, Haerizadeh F, Golden SS, et al** (2014) Broad-host-range vector system
1012 for synthetic biology and biotechnology in cyanobacteria. Nucleic Acids Res **42**: e136

Taylor GM, Hitchcock A, Heap JT (2021) Combinatorial assembly platform enabling engineering of genetically stable metabolic pathways in cyanobacteria. Nucleic Acids Res **49**: e123

Ungerer J, Pakrasi HB (2016) Cpf1 is a versatile tool for CRISPR genome editing across diverse species of cyanobacteria. Sci Rep **6**: 39681

Ungerer J, Wendt KE, Hendry JI, Maranas CD, Pakrasi HB (2018) Comparative genomics reveals the molecular determinants of rapid growth of the cyanobacterium Synechococcus elongatus UTEX 2973. Proc Natl Acad Sci USA **115**: E11761–E11770

Vasudevan R, Gale GAR, Schiavon AA, Puzorjov A, Malin J, Gillespie MD, Vavitsas K, Zulkower V, Wang B, Howe CJ, et al (2019) CyanoGate: a modular cloning suite for engineering cyanobacteria based on the plant MoClo syntax. Plant Physiol **180**: 39–55

Vento JM, Crook N, Beisel CL (2019) Barriers to genome editing with CRISPR in bacteria. J Ind Microbiol Biotechnol **46**: 1327–1341

Vogel AIM, Lale R, Hohmann-Marriott MF (2017) Streamlining recombination-mediated genetic engineering by validating three neutral integration sites in Synechococcus sp. PCC 7002. J Biol Eng **11**: 19

Wang S-Y, Li X, Wang S-G, Xia P-F (2023) Base editing for reprogramming cyanobacterium Synechococcus elongatus. Metab Eng **75**: 91–99

Wendt KE, Ungerer J, Cobb RE, Zhao H, Pakrasi HB (2016) CRISPR/Cas9 mediated targeted mutagenesis of the fast growing cyanobacterium Synechococcus elongatus UTEX 2973. Microb Cell Factories **15**: 115

Wilson KS, von Hippel PH (1995) Transcription termination at intrinsic terminators: the role of the RNA hairpin. Proc Natl Acad Sci USA **92**: 8793–8797

Włodarczyk A, Selão TT, Norling B, Nixon PJ (2020) Newly discovered Synechococcus sp. PCC 11901 is a robust cyanobacterial strain for high biomass production. Commun Biol **3**: 1–14

Xiao K, Yue X-H, Chen W-C, Zhou X-R, Wang L, Xu L, Huang F-H, Wan X (2018) Metabolic engineering for enhanced medium chain omega hydroxy fatty acid production in Escherichia coli. Front Microbiol **9**: 139

Yao L, Shabestary K, Björk SM, Asplund-Samuelsson J, Joensson HN, Jahn M, Hudson EP (2020) Pooled CRISPRi screening of the cyanobacterium Synechocystis sp PCC 6803 for enhanced industrial phenotypes. Nat Commun **11**: 1666

Yu J, Liberton M, Cliften PF, Head RD, Jacobs JM, Smith RD, Koppenaal DW, Brand JJ, Pakrasi HB (2015) Synechococcus elongatus UTEX 2973, a fast growing cyanobacterial chassis for biosynthesis using light and CO2. Sci Rep **5**: 8132

Zavřel T, Chmelík D, Sinetova MA, Červený J (2018) Spectrophotometric determination of phycobiliprotein content in cyanobacterium Synechocystis. J Vis Exp 58076

Zess EK, Begemann MB, Pfleger BF (2016) Construction of new synthetic biology tools for the control of gene expression in the cyanobacterium Synechococcus sp. strain PCC 7002. Biotechnol Bioeng **113**: 424–432

Zetsche B, Gootenberg JS, Abudayyeh OO, Slaymaker IM, Makarova KS, Essletzbichler P, Volz SE, Joung J, van der Oost J, Regev A, et al (2015) Cpf1 is a single RNA-guided endonuclease of a class 2 CRISPR-Cas system. Cell **163**: 759–771

Zhang A, Carroll AL, Atsumi S (2017) Carbon recycling by cyanobacteria: improving CO2 fixation through chemical production. FEMS Microbiol Lett **364**: fnx165

Zhou Y, Sun T, Chen Z, Song X, Chen L, Zhang W (2019) Development of a new biocontainment strategy in model cyanobacterium Synechococcus strains. ACS Synth Biol **8**: 2576–2584

1062 **FIGURE LEGENDS**

1063 **Figure 1.** Antibiotic susceptibility and characterisation of putative neutral integration sites in
1064 PCC 11901. **(A)** Susceptibility of wild-type PCC 11901 to increasing concentrations of
1065 common antibiotics. PCC 11901 wild-type cultures were inoculated at OD_{750} = 0.2 and
1066 grown in MAD medium as described in the Materials and Methods for 48 h. **(B)** The diagram
1067 illustrates the transformation strategy used to introduce antibiotic resistance (AbR) cassettes
1068 into each putative neutral site via homologous recombination. An integrative pUC19 plasmid
1069 vector was assembled using the CyanoGate MoClo system (Vasudevan et al., 2019) and 1 µg
1070 of each plasmid was transformed into wild-type (WT) PCC 11901 (see **Supplementary**
1071 **Table S2** for plasmid vectors). Colony images and numbers of mutants transformed with
1072 different AbR cassettes integrated into the *desB* neutral site. Colony counts were estimated by
1073 dividing the plate into nine sectors and taking the average colony counts of three sectors.
1074 Based on these results, we recommend concentrations of 100 µg mL^{-1} kanamycin, 25 µg mL^{-1}
1075 spectinomycin, 50 µg mL^{-1} gentamicin, 1.25 µg mL^{-1} erythromycin, and 5 µg mL^{-1}
1076 chloramphenicol for selection using the respective AbR cassettes. **(C)** Growth analysis of five
1077 putative neutral site mutants transformed with a spectinomycin resistance cassette (SpR) and
1078 grown in MAD medium as described in the Materials and Methods. Lowercase letters
1079 indicating significant difference ($P < 0.05$) are shown, as determined by ANOVA followed
1080 by Tukey's honestly significant difference tests. Error bars show the mean ±SEM of three
1081 biological replicates. Abbreviations: Cm, chloramphenicol; DF, Down Flank; Em,
1082 erythromycin; Gm, gentamicin; Km, kanamycin; Sp, spectinomycin; UF, Up Flank.

1083

1084 **Figure 2.** Transconjugation in PCC 11901. **(A)** Illustration showing conjugal transfer of a
1085 self-replicating RSF1010-based vector from an *E. coli* 'cargo strain' into PCC 11901. A
1086 transmissible helper plasmid is transferred from an *E. coli* helper strain to the cargo *E. coli*
1087 strain, which in turn aids the transfer of the mobilizable RSF1010 vector into the recipient
1088 PCC 11901. This series of steps is facilitated by the formation of conjugation pili where
1089 genetic material is transferred. **(B)** Representative image of PCC 11901 colony growth on
1090 membrane filters following selection on AD7 agar supplemented with 100 µg mL^{-1}
1091 kanamycin **(C)** pPMQAK1-T-based conjugants showed a typical dark green phenotype or a
1092 pale phenotype (red box) after streaking colonies from membranes filters onto agar media
1093 containing kanamycin. Pale colonies did not survive re-streaking. **(D)** Survival rates of
1094 transconjugants harbouring RSF1010-based vectors selected for with kanamycin
1095 (pPMQAK1-T and pPMQAK1-T-eYFP) or spectinomycin (pPMQSK1-1, pPMQSK1-1-

eYFP and pPMQSK1-1-Cas12a). **(E)** Growth comparison of transconjugant and transformant strains. **(F)** Fluorescence of transconjugant and transformant strains expressing eYFP measured at 24 h. **(G)** Growth comparison for transformant and transconjugant strains expressing eYFP. For (E), (F) and (G) lowercase letters indicating significant difference ($P < 0.05$) are shown, as determined by ANOVA followed by Tukey's honestly significant difference tests. Error bars show the mean ±SEM of three biological replicates.

Figure 3. Characterisation of constitutive promoters and transcriptional terminators in PCC 11901. **(A)** Expression levels of eYFP driven by constitutive promoters integrated into the *mrr* neutral site, or **(B)** on the self-replicating pPMQAK1-T vector. **(C)** Correlation analysis of the expression levels of constitutive promoters integrated into the *mrr* neutral site or on a pPMQAK1-T vector. **(D)** Termination efficiency (TE) values for terminator sequences calculated as in Gale et al. (2021). Error bars represent the mean ±SEM of three biological replicates, each calculated from 10,000 individual cells. Abbreviations: P_{const}, constitutive promoter; T_{term}, transcriptional terminator.

Figure 4. Evaluation of three inducible promoter systems in PCC 11901**.** Overview of the genetic components and dose-response expression levels of eYFP 24 h after induction with increasing concentrations of their respective substrate for the **(A, B)** L-rhamnose-inducible promoter RhaS/P_{rhaBAD} fluorescent reporter system, **(C, D)** theophylline-inducible promoter P_{trcE*} fluorescent reporter system and **(E, F)** DAPG-inducible PhlF/P_{phlF} fluorescent reporter system. The eYFP expression level for the constitutive P_{cpc560} promoter (pPMQAK1-T-eYFP, **Figure 2F**) is included for comparison. Error bars show the mean ±SEM of three biological replicates.

Figure 5. Inducible CRISPR interference (CRISPRi) for conditional knockdown of gene expression in PCC 11901. **(A)** Overview of the approaches used to test dCas9 functionality by targeting an eYFP expression cassette integrated into the *mrr* neutral site (bottom schematic) using sgRNAs targeting four different sites neighbouring a dCas9 protospacer adjacent motif sequence 5'-NGG-3' in the eYFP open reading frame (Vasudevan et al., 2019). **(B-E)** eYFP fluorescence of plasmid vectors carrying sgRNAs with and without a constitutively expressed (P_{J23113}) or inducible (RhaS/P_{rhaBAD}, PhlF/P_{phlF} and P_{trcE*}) dCas9 and a strain carrying no sgRNA as a control. **(F)** Illustration of the *cpc* operon and the sgRNA target site (red bar, see **Supplementary Table S3** for sequence) in *cpcB* (c-phycocyanin

subunit β, FEK30_15275). **(G)** The *cpcB* CRISPRi strains with and without inducer after 24 h of growth in MAD medium. **(H)** Growth of the *cpcB* CRISPRi strains with and without inducer over 48 h. **(I)** Absorbance spectra of PBS extracts from strains in (G). **(J)** Illustration of the sgRNA target site in *nblA* (nonbleaching A, FEK30_13550). **(K)** The *nblA* CRISPRi strains with and without inducer after 24 h of growth in MAD medium without nitrogen. **(L)** Growth of the *nblA* CRISPRi strains with and without inducer over 48 h. **(M)** Absorbance spectra of PBS extracts from strains in (K). Error bars show the mean ±SEM of three biological replicates.

Figure 6. Genome editing of PCC 11901 with CRISPR-Cas12a using a double homologous recombination approach. **(A)** The editing strategy relies on an RSF1010-based editing vector (pC1.509, **Supplementary Figure S1**) and a pUC19 suicide vector. Transformation of the pUC19 suicide vector into an 'editing strain' carrying pC1.509 results in (1) HR with pC1.509 to deliver the sgRNA(s) and GmR (components in blue) and (2) HR with the target genomic locus to deliver a template for homology directed repair (components in purple). Subsequent DAPG-induction of Cas12a results in cleavage of the target locus (in grey), leaving only edited copies of the genome (in purple) intact (for a detailed methodology and protocols see **Supplementary Figure S7** and **S8**). **(B,C)** Demonstration of single genome editing through markerless insertion of eYFP into the *mrr* locus and mCherry into the *aquI* locus, respectively. (**D**) Iterative genome editing through markerless insertion of mCherry into the *aquI* locus of the Δ*mrr*::eYFP strain. (**E**) Multiplexed genome editing through simultaneous insertion of eYFP and mCherry into the *mrr* and *aquI* locus, respectively. (F) Demonstration of curing of the RSF1010 editing vector using a self-targeting sgRNA.

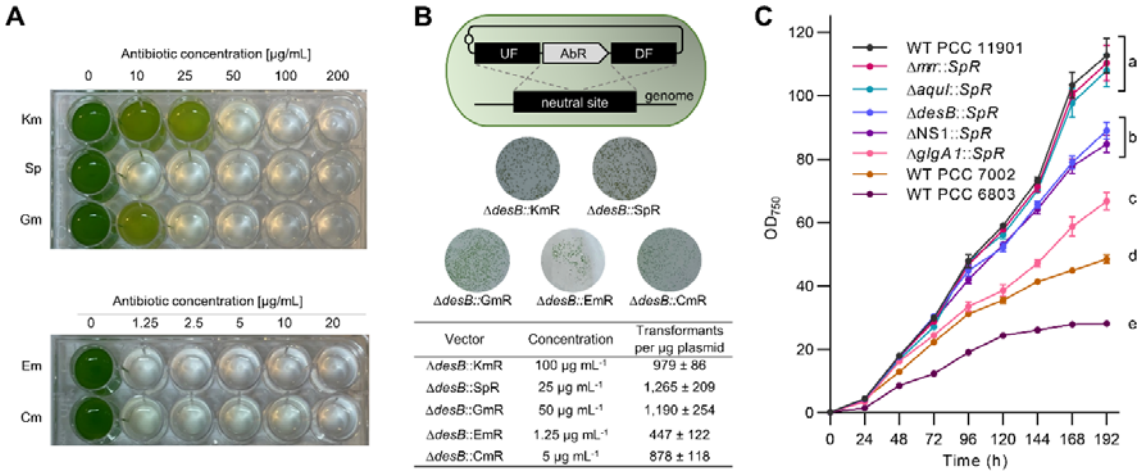

Vector	Concentration	Transformants per µg plasmid
Δ*desB*::KmR	100 µg mL^{-1}	979 ± 86
Δ*desB*::SpR	25 µg mL^{-1}	1,265 ± 209
Δ*desB*::GmR	50 µg mL^{-1}	1,190 ± 254
Δ*desB*::EmR	1.25 µg mL^{-1}	447 ± 122
Δ*desB*::CmR	5 µg mL^{-1}	878 ± 118

Figure 1. Antibiotic susceptibility and characterisation of putative neutral integration sites in PCC 11901. **(A)** Susceptibility of wild-type PCC 11901 to increasing concentrations of common antibiotics. PCC 11901 wild-type cultures were inoculated at OD_{750} = 0.2 and grown in MAD medium as described in the Materials and Methods for 48 h. **(B)** The diagram illustrates the transformation strategy used to introduce antibiotic resistance (AbR) cassettes into each putative neutral site via homologous recombination. An integrative pUC19 plasmid vector was assembled using the CyanoGate MoClo system (Vasudevan et al., 2019) and 1 µg of each plasmid was transformed into wild-type (WT) PCC 11901 (see **Supplementary Table S2** for plasmid vectors). Colony images and numbers of mutants transformed with different AbR cassettes integrated into the *desB* neutral site. Colony counts were estimated by dividing the plate into nine sectors and taking the average colony counts of three sectors. Based on these results, we recommend concentrations of 100 µg mL^{-1} kanamycin, 25 µg mL^{-1} spectinomycin, 50 µg mL^{-1} gentamicin, 1.25 µg mL^{-1} erythromycin, and 5 µg mL^{-1} chloramphenicol for selection using the respective AbR cassettes. **(C)** Growth analysis of five putative neutral site mutants transformed with a spectinomycin resistance cassette (SpR) and grown in MAD medium as described in the Materials and Methods. Lowercase letters indicating significant difference ($P < 0.05$) are shown, as determined by ANOVA followed by Tukey's honestly significant difference tests. Error bars show the mean ±SEM of three biological replicates. Abbreviations: Cm, chloramphenicol; DF, Down Flank; Em, erythromycin; Gm, gentamicin; Km, kanamycin; Sp, spectinomycin; UF, Up Flank.

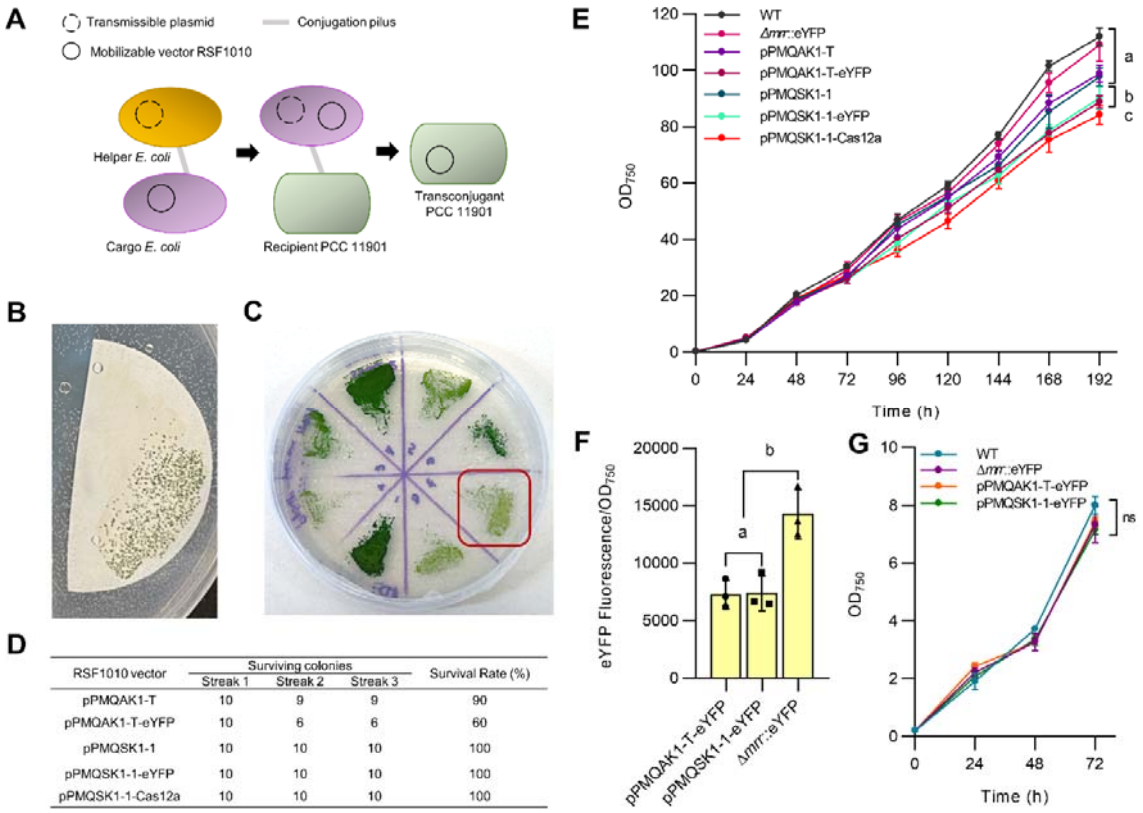

RSF1010 vector	Surviving colonies			Survival Rate (%)
	Streak 1	Streak 2	Streak 3	
pPMQAK1-T	10	9	9	90
pPMQAK1-T-eYFP	10	6	6	60
pPMQSK1-1	10	10	10	100
pPMQSK1-1-eYFP	10	10	10	100
pPMQSK1-1-Cas12a	10	10	10	100

Figure 2. Transconjugation in PCC 11901. **(A)** Illustration showing conjugal transfer of a self-replicating RSF1010-based vector from an *E. coli* 'cargo strain' into PCC 11901. A transmissible helper plasmid is transferred from an *E. coli* helper strain to the cargo *E. coli* strain, which in turn aids the transfer of the mobilizable RSF1010 vector into the recipient PCC 11901. This series of steps is facilitated by the formation of conjugation pili where genetic material is transferred. **(B)** Representative image of PCC 11901 colony growth on membrane filters following selection on AD7 agar supplemented with 100 µg mL^{-1} kanamycin **(C)** pPMQAK1-T-based conjugants showed a typical dark green phenotype or a pale phenotype (red box) after streaking colonies from membranes filters onto agar media containing kanamycin. Pale colonies did not survive re-streaking. **(D)** Survival rates of transconjugants harbouring RSF1010-based vectors selected for with kanamycin (pPMQAK1-T and pPMQAK1-T-eYFP) or spectinomycin (pPMQSK1-1, pPMQSK1-1-eYFP and pPMQSK1-1-Cas12a). **(E)** Growth comparison of transconjugant and transformant strains. **(F)** Fluorescence of transconjugant and transformant strains expressing eYFP measured at 24 h. **(G)** Growth comparison for transformant and transconjugant strains expressing eYFP. For (E), (F) and (G) lowercase letters indicating significant difference (P <

1194 0.05) are shown, as determined by ANOVA followed by Tukey's honestly significant
1195 difference tests. Error bars show the mean ±SEM of three biological replicates.
1196

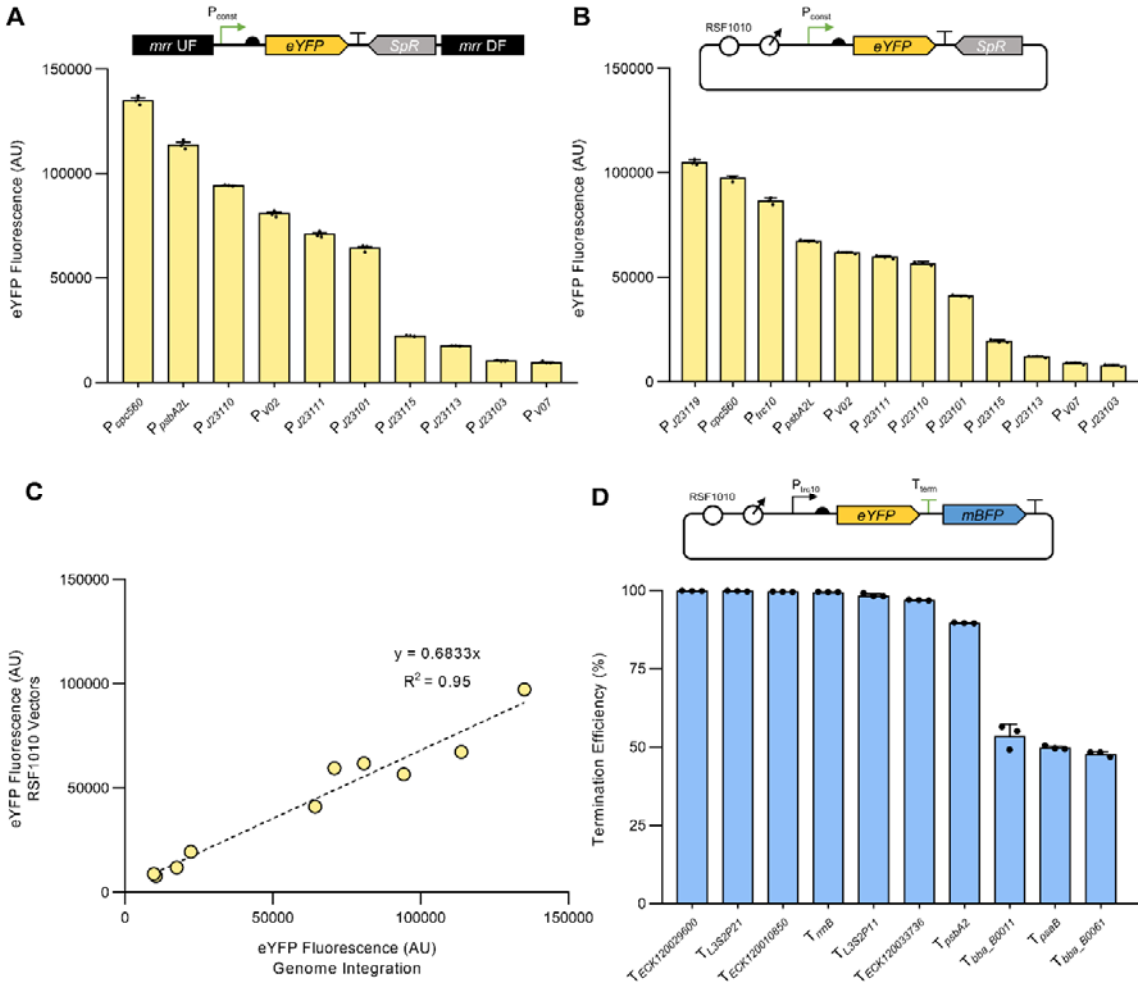

Figure 3. Characterisation of constitutive promoters and transcriptional terminators in PCC 11901. **(A)** Expression levels of eYFP driven by constitutive promoters integrated into the *mrr* neutral site, or **(B)** on the self-replicating pPMQAK1-T vector. **(C)** Correlation analysis of the expression levels of constitutive promoters integrated into the *mrr* neutral site or on a pPMQAK1-T vector. **(D)** Termination efficiency (TE) values for terminator sequences calculated as in Gale et al. (2021). Error bars represent the mean ±SEM of three biological replicates, each calculated from 10,000 individual cells. Abbreviations: P_{const}, constitutive promoter; T_{term}, transcriptional terminator.

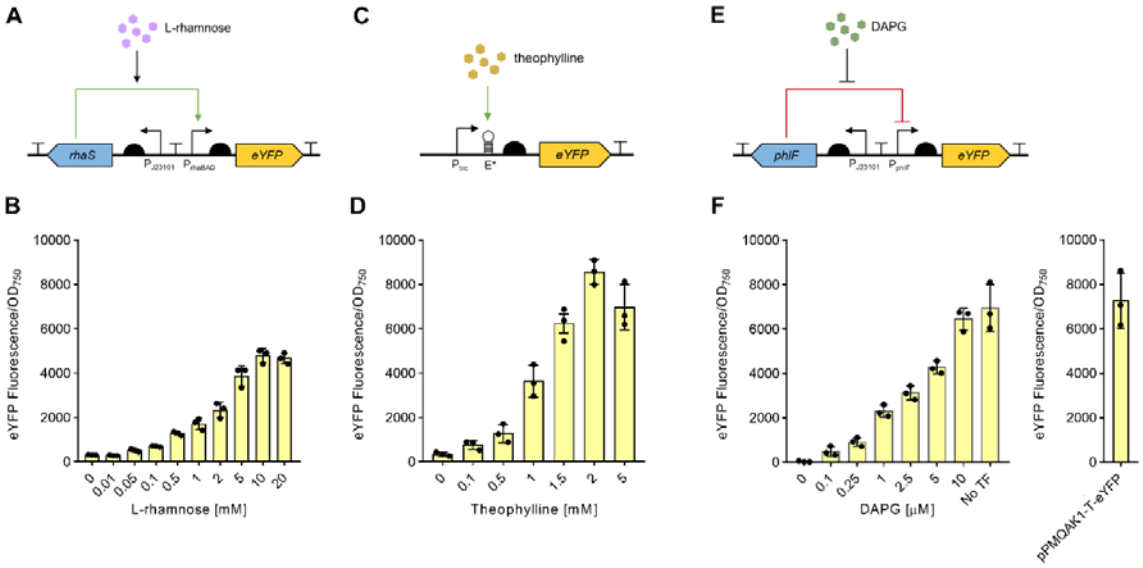

Figure 4. Evaluation of three inducible promoter systems in PCC 11901**.** Overview of the genetic components and dose-response expression levels of eYFP 24 h after induction with increasing concentrations of their respective substrate for the **(A, B)** L-rhamnose-inducible promoter RhaS/P_{rhaBAD} fluorescent reporter system, **(C, D)** theophylline-inducible promoter P_{trcE*} fluorescent reporter system and **(E, F)** DAPG-inducible PhlF/P_{phlF} fluorescent reporter system. The eYFP expression level for the constitutive P_{cpc560} promoter (pPMQAK1-T-eYFP, **Figure 2F**) is included for comparison. Error bars show the mean ±SEM of three biological replicates.

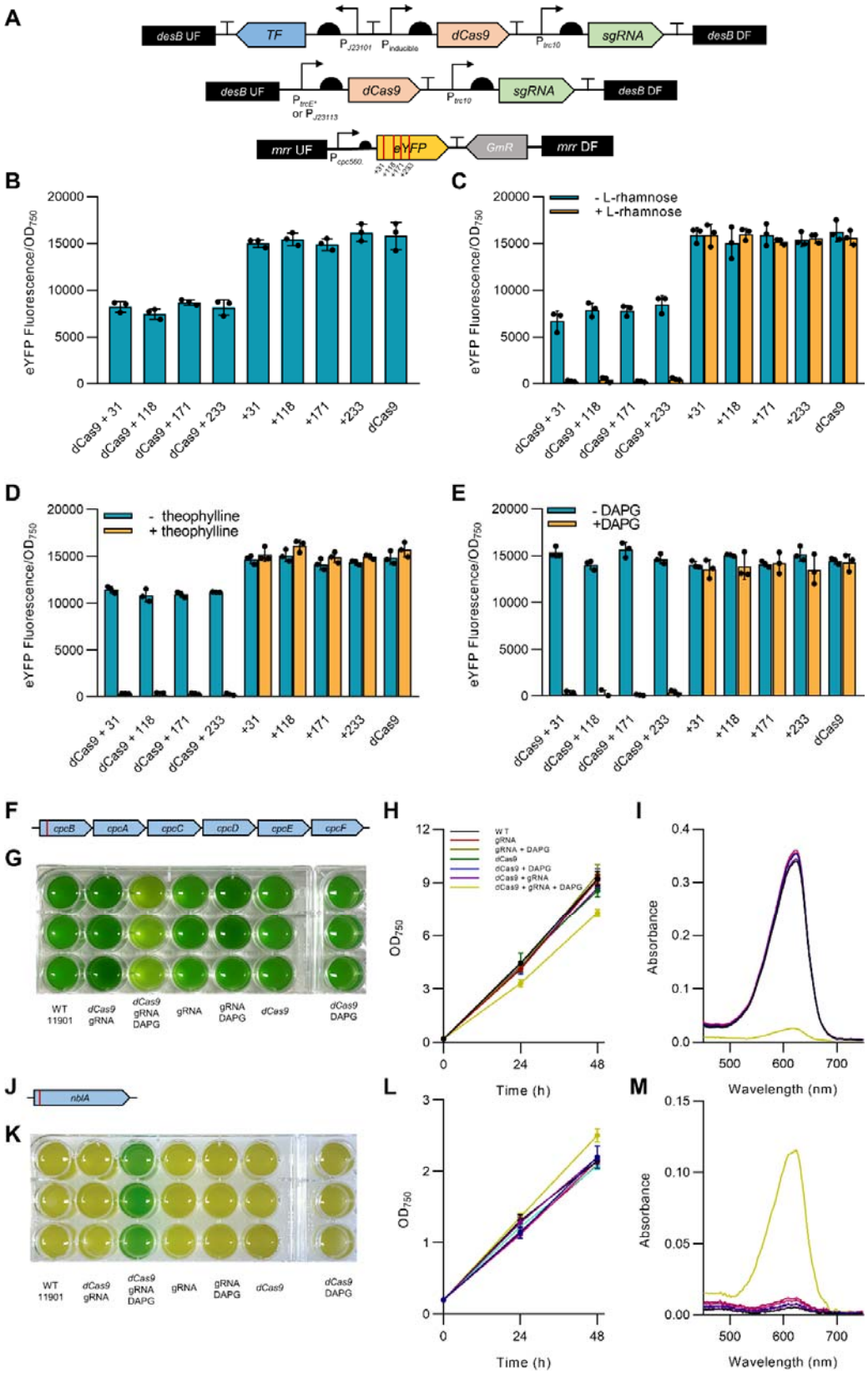

Figure 5. Inducible CRISPR interference (CRISPRi) for conditional knockdown of gene expression in PCC 11901. **(A)** Overview of the approaches used to test dCas9 functionality

1221 by targeting an eYFP expression cassette integrated into the *mrr* neutral site (bottom
1222 schematic) using sgRNAs targeting four different sites neighbouring a dCas9 protospacer
1223 adjacent motif sequence 5'-NGG-3' in the eYFP open reading frame (Vasudevan et al.,
1224 2019). **(B-E)** eYFP fluorescence of plasmid vectors carrying sgRNAs with and without a
1225 constitutively expressed (P_{J23113}) or inducible (RhaS/P_{rhaBAD}, PhlF/P_{phlF} and P_{trcE*}) dCas9 and
1226 a strain carrying no sgRNA as a control. **(F)** Illustration of the *cpc* operon and the sgRNA
1227 target site (red bar, see **Supplementary Table S3** for sequence) in *cpcB* (c-phycocyanin
1228 subunit β, FEK30_15275). **(G)** The *cpcB* CRISPRi strains with and without inducer after 24
1229 h of growth in MAD medium. **(H)** Growth of the *cpcB* CRISPRi strains with and without
1230 inducer over 48 h. **(I)** Absorbance spectra of PBS extracts from strains in (G). **(J)** Illustration
1231 of the sgRNA target site in *nblA* (nonbleaching A, FEK30_13550). **(K)** The *nblA* CRISPRi
1232 strains with and without inducer after 24 h of growth in MAD medium without nitrogen. **(L)**
1233 Growth of the *nblA* CRISPRi strains with and without inducer over 48 h. **(M)** Absorbance
1234 spectra of PBS extracts from strains in (K). Error bars show the mean ±SEM of three
1235 biological replicates.

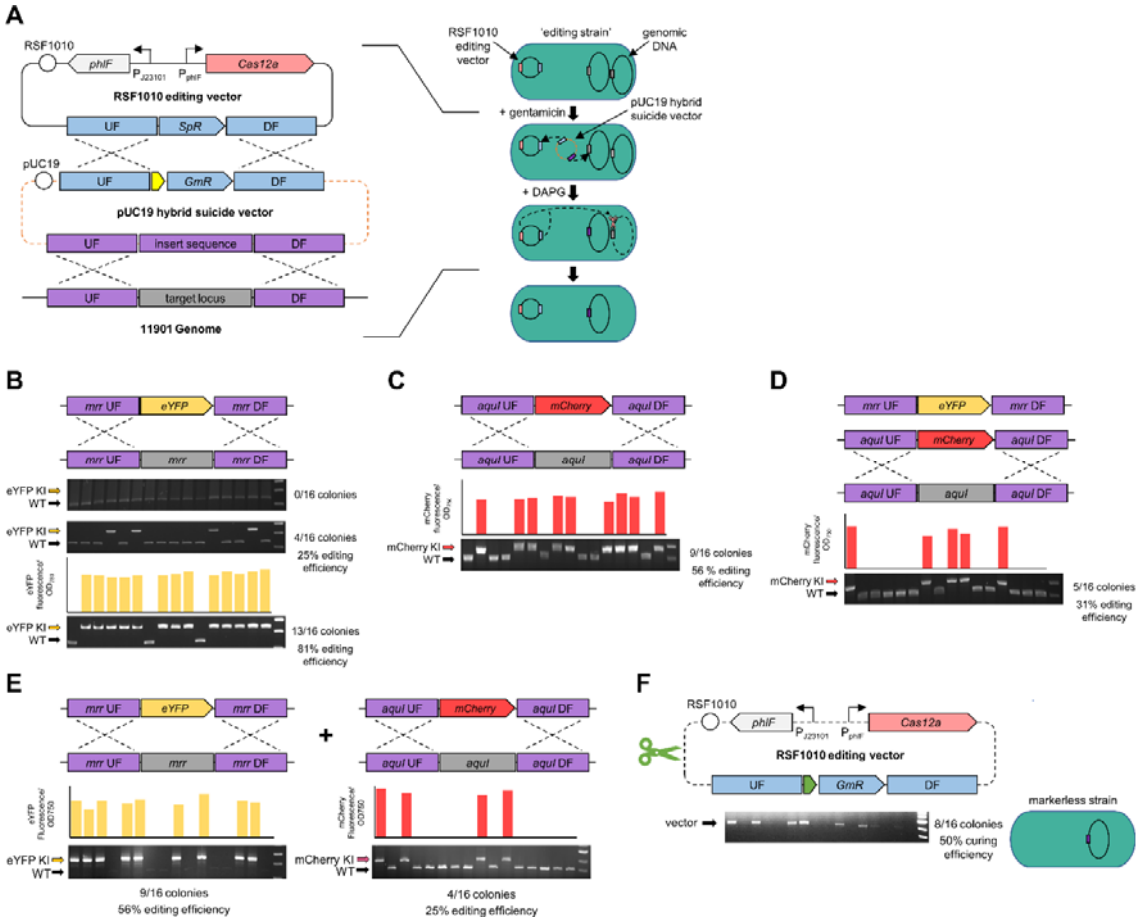

Figure 6. Genome editing of PCC 11901 with CRISPR-Cas12a using a double homologous recombination approach. **(A)** The editing strategy relies on an RSF1010-based editing vector (pC1.509, **Supplementary Figure S1**) and a pUC19 suicide vector. Transformation of the pUC19 suicide vector into an 'editing strain' carrying pC1.509 results in (1) HR with pC1.509 to deliver the sgRNA(s) and GmR (components in blue) and (2) HR with the target genomic locus to deliver a template for homology directed repair (components in purple). Subsequent DAPG-induction of Cas12a results in cleavage of the target locus (in grey), leaving only edited copies of the genome (in purple) intact (for a detailed methodology and protocols see **Supplementary Figure S7** and **S8**). **(B,C)** Demonstration of single genome editing through markerless insertion of eYFP into the *mrr* locus and mCherry into the *aquI* locus, respectively. (**D**) Iterative genome editing through markerless insertion of mCherry into the *aquI* locus of the Δ*mrr*::eYFP strain. (**E**) Multiplexed genome editing through simultaneous insertion of eYFP and mCherry into the *mrr* and *aquI* locus, respectively. (F) Demonstration of curing of the RSF1010 editing vector using a self-targeting sgRNA.

1252 **Supplementary Table S1.** Table of all new CyanoGate-compatible parts generated in this work.

1253

No.	Vector ID	Part name	Level	5' overhang	3' overhang	Backbone	Domesticated	Selection	Notes	References
Acceptors										
Level T										
1	pCAT.482	pPMQSK1-T	T	TGCC	GGGA	pPMQSK	yes	SpR/KmR	Modified BioBrick vector, RSF1010-derived ori.	Huang et al., 2010
Level 1										
1	pCA1.339	pPMQSK1-1	1	GGAG	GGGA	pPMQSK	yes	SpR/KmR	Modified BioBrick vector, RSF1010-derived ori.	Huang et al., 2010
Level 0										
1	pCA0.421	sgRNA acceptor	0	AATG	AGGT	pICH41258	no	SpR	Acceptor of sgRNA(s) for CRISPR-Cas12a gene editing	this study
Insertion Sites										
1	pC0.378	*desB* Down Flank	0	GCTT	CGCT	pICH41276	no	SpR	*Synechococcus* sp. PCC 11901 sequence downstream of FEK30_04840.	Mills et al., 2022 Vogel et al., 2017
2	pC0.385	*desB* Up Flank	0	GGAG	AATG	pICH41295	yes	SpR	*Synechococcus* sp. PCC 11901 sequence upstream of FEK30_04840.	Mills et al., 2022 Vogel et al., 2017
3	pC0.386	*glgA1* Up Flank	0	GGAG	AATG	pICH41295	no	SpR	*Synechococcus* sp. PCC 11901 sequence upstream of FEK30_14880.	Sengupta et al., 2020, Mittermair et al., 2021
4	pC0.387	*glgA1* Down Flank	0	GCTT	CGCT	pICH41276	no	SpR	*Synechococcus* sp. PCC 11901 sequence downstream of FEK30_14880.	Sengupta et al., 2020, Mittermair et al., 2021
5	pC0.388	*mrr* Up Flank	0	GGAG	AATG	pICH41295	yes	SpR	*Synechococcus* sp. PCC 11901 sequence upstream of FEK30_09380.	this study
6	pC0.389	*mrr* Down Flank	0	GCTT	CGCT	pICH41276	yes	SpR	*Synechococcus* sp. PCC 11901 sequence downstream of FEK30_09380.	this study
7	pC0.419	*aquI* Down Flank	0	GCTT	CGCT	pICH41276	no	SpR	*Synechococcus* sp. PCC 11901 sequence downstream of FEK30_10065.	this study
8	pC0.420	*aquI* Up Flank	0	GGAG	AATG	pICH41295	no	SpR	*Synechococcus* sp. PCC 11901 sequence upstream of FEK30_10065.	this study
9	pC0.425	RSF1010 Up Flank	0	GGAG	AATG	pICH41295	no	SpR	RSF1010 upstream homology sequence	this study

10	pC0.426	RSF1010 Down Flank	0	GCTT	CGCT	pICH41276	no	SpR	RSF1010 downstream homology sequence	this study
11	pC0.437	NS1 Up Flank	0	GGAG	AATG	pICH41295	no	SpR	*Synechococcus* sp. PCC 11901 sequence upstream of an intergenic region of 185bp between FEK30_11550 and FEK30_11555)	Bernhards et al., 2022
12	pC0.438	NS1 Down Flank	0	GCTT	CGCT	pICH41276	yes	SpR	*Synechococcus* sp. PCC 11901 sequence downstream of an intergenic region of 185bp between FEK30_11550 and FEK30_11555)	Bernhards et al., 2022
Promoters										
1	pC0 422	P_{rhaBAD}	0	GGAG	AATG	pICH41295	no	SpR	L-rhamnose inducible promoter	Kelly et al., 2018
2	pC0.423	P_{phlF}	0	GGAG	AATG	pICH41295	no	SpR	2,4-diacetylphloroglucinol inducible promoter from *Pseudomonas fluorescens*	Meyer et al., 2019
3	pC0.394	P_{trcE*}	0	GGAG	AATG	pSB4K5	no	SpR	theophylline responsive riboswitch E*	Nakahira et al., 2014
Parts										
1	pC0.393	Ab^{R}Gent	0	AGGT	GCCT	pICH41264	no	SpR/ GmR	Gentamicin resistance cassette	this study
2	pC0.391	Cas12a	0			pICH41308	no	SpR	Cas12a/Cpf1 from Francisella novicida	Zetsche et al., 2015
Other										
1	pC1.509	Cas12a editing vector	1			pPMQSK1-1	no	SpR	Editing vector for CRISPR-Cas12a gene editing (see Figure 6 for details)	this study
2	pC1.530	Curing vector (GmR) for editing strain	1			pPMQSK1-1	no	SpR	Curing vector with sgRNA and GmR for removing Cas12a editing vector (see Figure 6x for details)	this study

Additional references

Zetsche, B., Gootenberg, J. S., Abudayyeh, O. O., Slaymaker, I. M., Makarova, K. S., Essletzbichler, P., Volz, S. E., Joung, J., van der Oost, J., Regev, A., Koonin, E. V., & Zhang, F. (2015). Cpf1 Is a Single RNA-Guided Endonuclease of a Class 2 CRISPR-Cas System. *Cell*, *163*(3), 759–771. https://doi.org/10.1016/j.cell.2015.09.038

1254 **Supplementary Table S2.** All plasmids made and used in this study. See 'Supplementary
1255 Table S2 - Plasmids (all).xlsx'. RSF1010 vectors used for promoter and terminator
1256 characterisations in Figure 3B and 3C, respectively, have been published previously
1257 (Vasudevan et al., 2019; Gale et al., 2021).
1258
1259 **Supplementary Table S3.** Primer and sgRNA oligonucleotides used in this study. See
1260 'Supplementary Table S3 - Primer and sgRNA oligonucleotides.xlsx'.
1261
1262 **Supplementary Data S1.** Sequence maps (.gb files) for plasmid vectors in Supplementary
1263 Table S1. See 'Supplementary Data S1.zip'.
1264

A

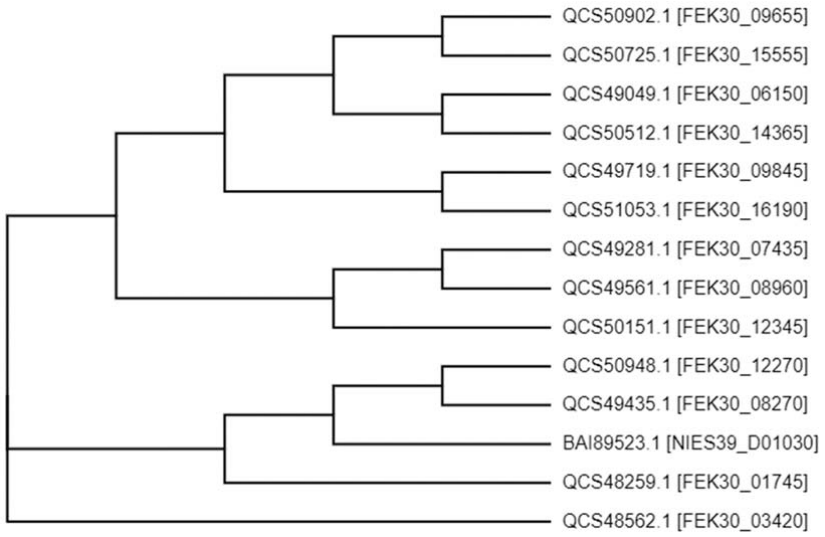

B

```
Aligned_sequences: 2
# 1: BAI89523.1
# 2: QCS49435.1
# Matrix: EBLOSUM62
# Gap_penalty: 10.0
# Extend_penalty: 0.5
# Length: 219
# Identity:      46/219 (21.0%)
# Similarity:    68/219 (31.1%)
# Gaps:          87/219 (39.7%)
# Score: 100.0

CLUSTAL O(1.2.4) multiple sequence alignment

BAI89523.1          MRIINLSPNNQNHIHQAATLLV-AEFRENWPNAWPTYERGLAEVMESFGDDRVNLVAVDE   59
QCS49435.1          MNKISDCSNILFSVDKARVDLVQLQALFNATAFWA-RERSLADLETAIA-YSDPVVTVWD   58
                    *. *. . *    :.:* . **  :   *    *   **.**::  ::.     :*:* :

BAI89523.1          NDNLLGWIGGIS--QYQGHVWELHPLVVKSDYQGLGIGRKLVANLEDYVRSQGGLTLWLG   117
QCS49435.1          GDRLIGFTRGTSDGVFRATVWD---VVIHPDYQGLGLGRKLVETLISHPRMCRVERVYLM   115
                    .*.*:*:  * *   ::. **:   :*:: ******:***** .* .: *      ::*

BAI89523.1          TDDENNLTSLSGVELYPHFLENIANIKNHGRHPYEFYQKCGFVIMGVVPDANGIGKPDIL   177
QCS49435.1          TTH----------------------------QQTFYERIGFKENATTTM----------   136
                    * .                                **:: **   ...

BAI89523.1          MAKSLRIDNHPKSN-------------     191
QCS49435.1          ---VLHNHEHPISVITCAVEETAPLPA     160
                       *: .:** *
```

Supplementary Figure S1. Analysis of putative Gcn5-related N-acetyltransferase (GNAT) family genes in PCC 11901. **(A)** Phylogenetic tree of 13 GNAT family proteins in PCC 11901 and the aminoglycoside acetyltransferase from *Arthrospira platensis* (BAI89523.1)

1289 (built by Clustal Omega (EMBL-EBI)). **(B)** Sequence alignment and scores between
1290 BAI89523.1 and a putative aminoglycoside acetyltransferase from PCC 11901
1291 (QCS49435.1). The conserved coenzyme A binding pocket is highlighted in yellow. The
1292 alignment was performed in EMBOSS Needle.

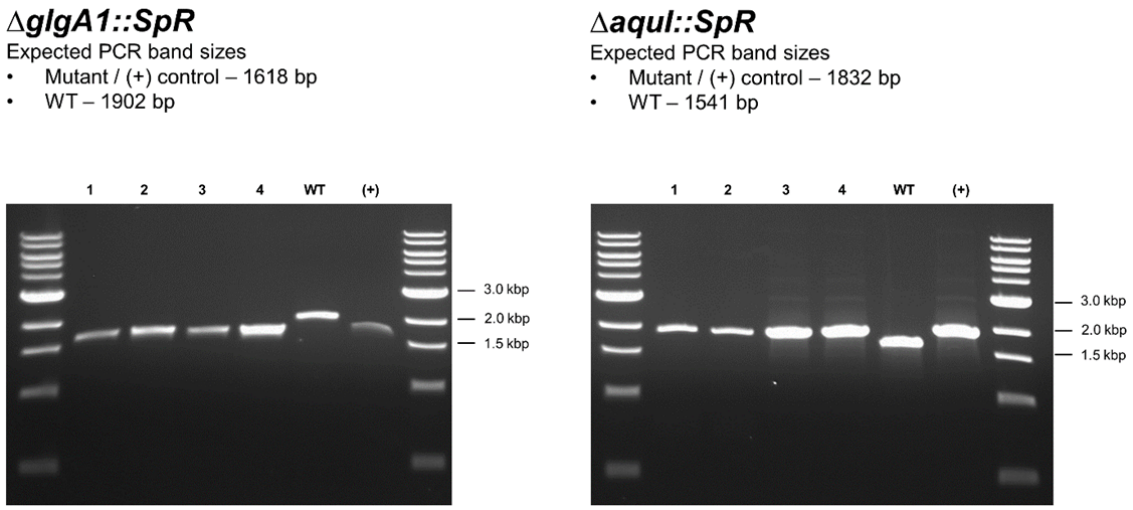

Supplementary Figure S2. Representative PCR-based segregation analysis of PCC 11901 transformants targeting neutral sites *glgA1* and *aquI*. Electrophoresis gel profiles are shown for four independent transformant colonies after one round of re-streaking on selective agar. Full segregation for each transformant is demonstrated by the presence of amplicons showing insertion of the SpR cassette at the *glgA1* (1,618 bp) and *aquI* (1,832 bp) loci and the absence of a respective wild-type (WT) amplicon (1,902 bp for *glgA1* and 1,541 bp for *aquI*). Amplicons from each transformation plasmid (+) are included as positive controls.

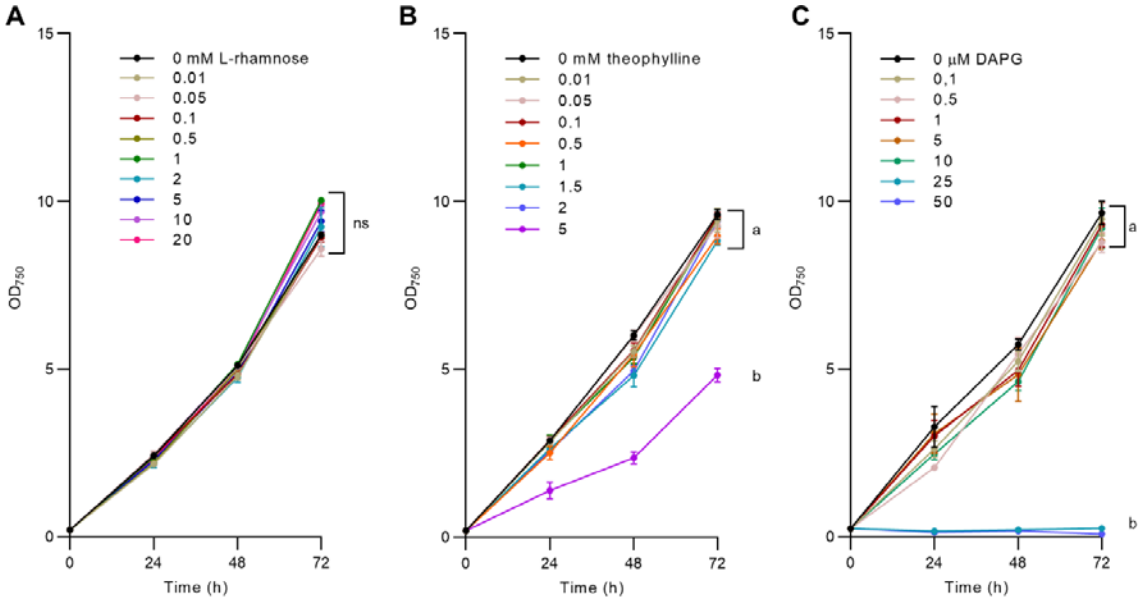

Supplementary Figure S3. Growth of PCC 11901 with varying doses of small molecule inducers. Growth of wild-type PCC 11901 in increasing concentrations of **(A)** L-rhamnose, **(B)** theophylline, and **(C)** DAPG over 72 h. Error bars represent the mean ±SEM of three biological replicates.

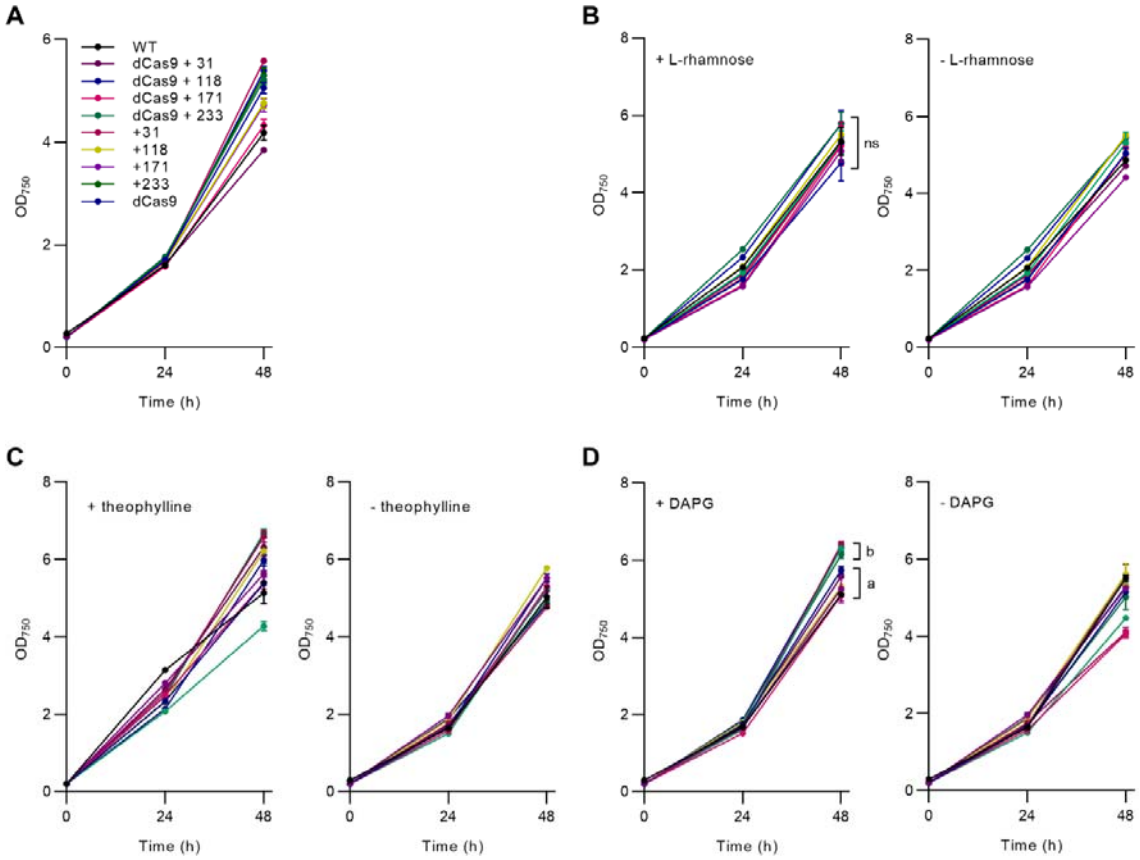

Supplementary Figure S4. Growth analysis of CRISPRi-dCas9 strains targeting eYFP. **(A)** Growth of P_{J23113} CRISPRi strains in MAD medium. **(B)** Growth of RhaS/P_{rhaBAD} CRISPRi strains in the presence or absence of 10 mM L-rhamnose. **(C)** Growth of P_{trcE*} CRISPRi strains in the presence or absence of 2 mM theophylline. **(D)** Growth of PhlF/P_{phlF} CRISPRi strains in the presence or absence of 10 µM DAPG. Error bars represent mean ±SEM of three biological replicates.

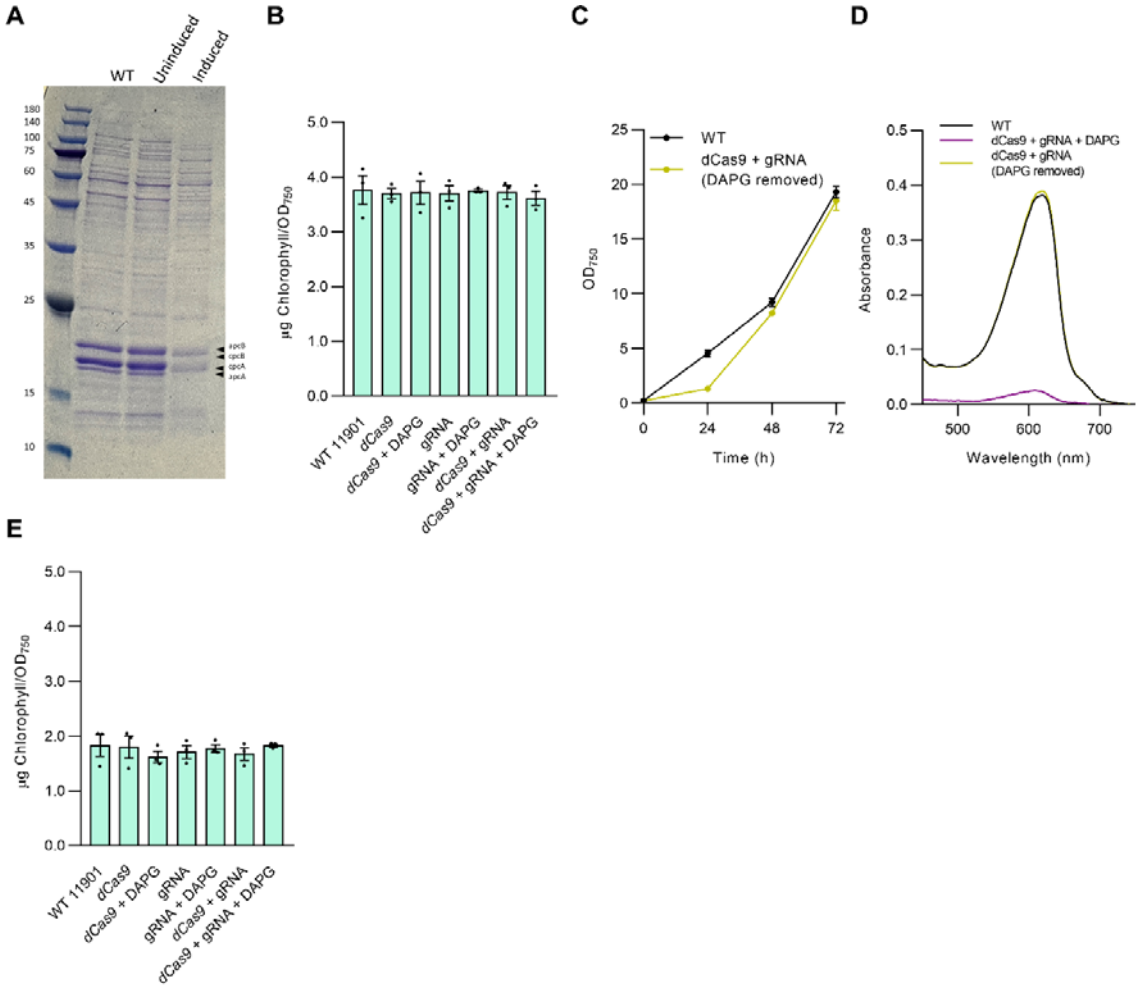

Supplementary Figure S5. Analysis of CRISPRi-dCAs9 strains targeting *cpcB* and *nblA*. **(A)** Coomassie-stained SDS-PAGE gel of PBS extracts from the *cpcB* CRISPRi strain carrying both sgRNA and dCas9 in the absence (uninduced) or presence (induced) of 10 µM DAPG. Arrows indicate the bands for *apcB* (18.7 kdA), *cpcB* (18.1 kdA), *cpcA* (17.6 kdA) and *apcA* (17.3 kdA). **(B)** Chlorophyll contents of the *cpcB* CRISPRi strains. **(C)** Growth of the *cpcB* CRISPRi strain carrying both sgRNA and dCas9 in comparison to wild-type PCC 11901 following removal of DAPG. **(D)** Absorbance spectra of PBS extracts following removal of DAPG at 48 h. **(E)** Chlorophyll contents of *nblA* CRISPRi strains. Error bars show the mean ±SEM of three biological replicates for B, C and E.

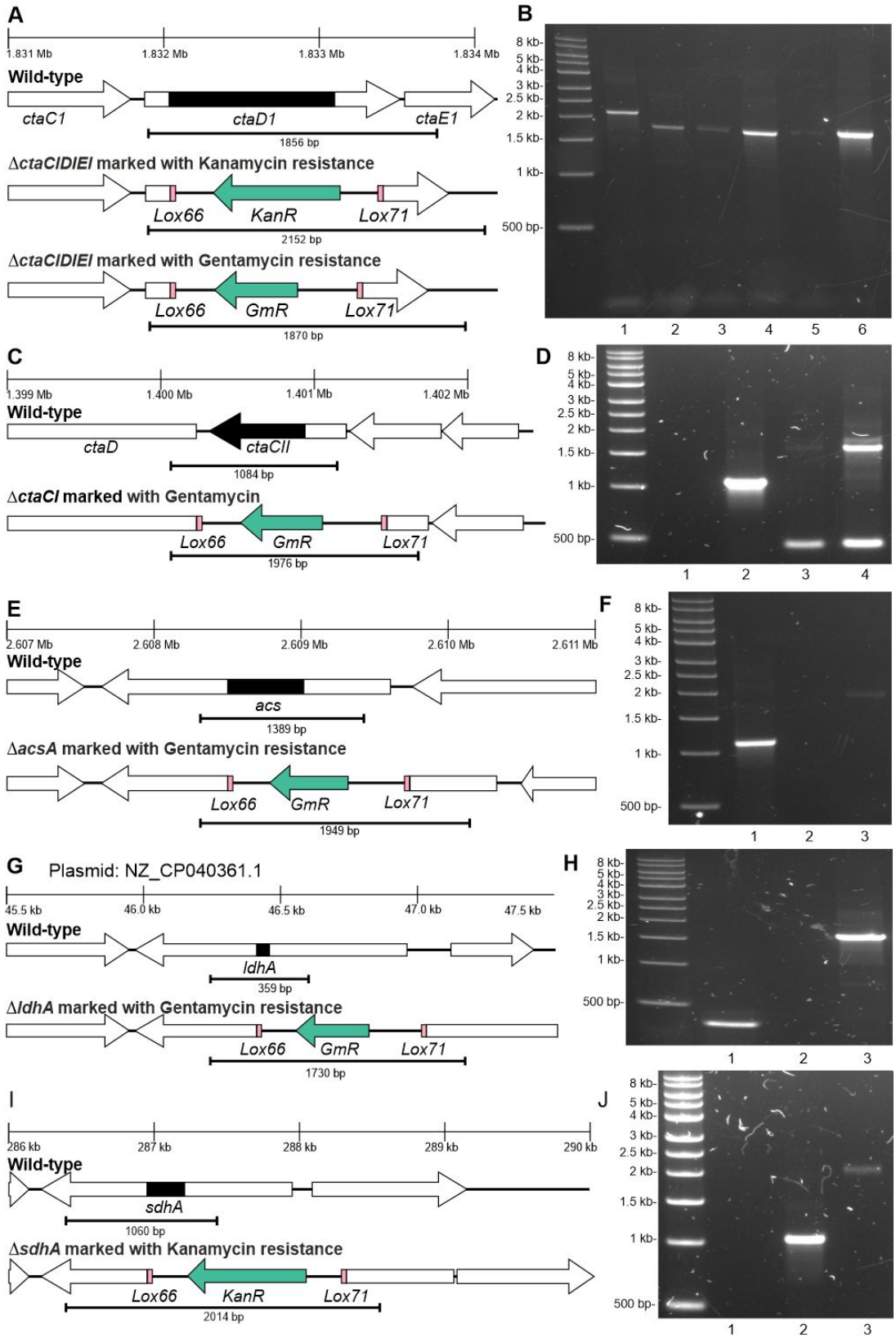

Supplementary Figure S6. Attempted generation of markerless mutants using the CRE-Lox system. Schematic representations of locus location in the PCC 11901 genome (top) and the

1332 wild-type (middle) and marked knockout (KO, bottom) profiles expected in the **(A)** *ctaDIEI*,
1333 **(C)** *ctaCII*, **(E)** *acs*, **(G)** *ldhA* and **(I)** *sdhA* strains following amplification with primers
1334 flanking the deleted sequence. Regions deleted in the mutant strains are shaded in black.
1335 Amplification of genomic DNA in: **(B)** Δ*ctaDIEI* KmR marked KO (lane 1); Δ*ctaDIEI* GmR
1336 marked KO (lanes 2-5); WT (lane 6); **(D)** negative control (lane 1); WT (lane 2); Δ*ctaCII*
1337 GmR marked KO (lanes 3-4); **(F)** WT (lane 1); negative control (lane 2); Δ*acs* GmR marked
1338 KO (lane 3); **(H)** WT (lane 1); negative control (lane 2); Δ*ldhA* GmR marked KO (lane 3);
1339 **(J)** negative control (lane 1); WT (lane 2); Δ*sdhA* KmR marked KO (lane 3). Δ*ctaDIEI* GmR
1340 marked KOs were sequenced to confirm the correct KO profile.

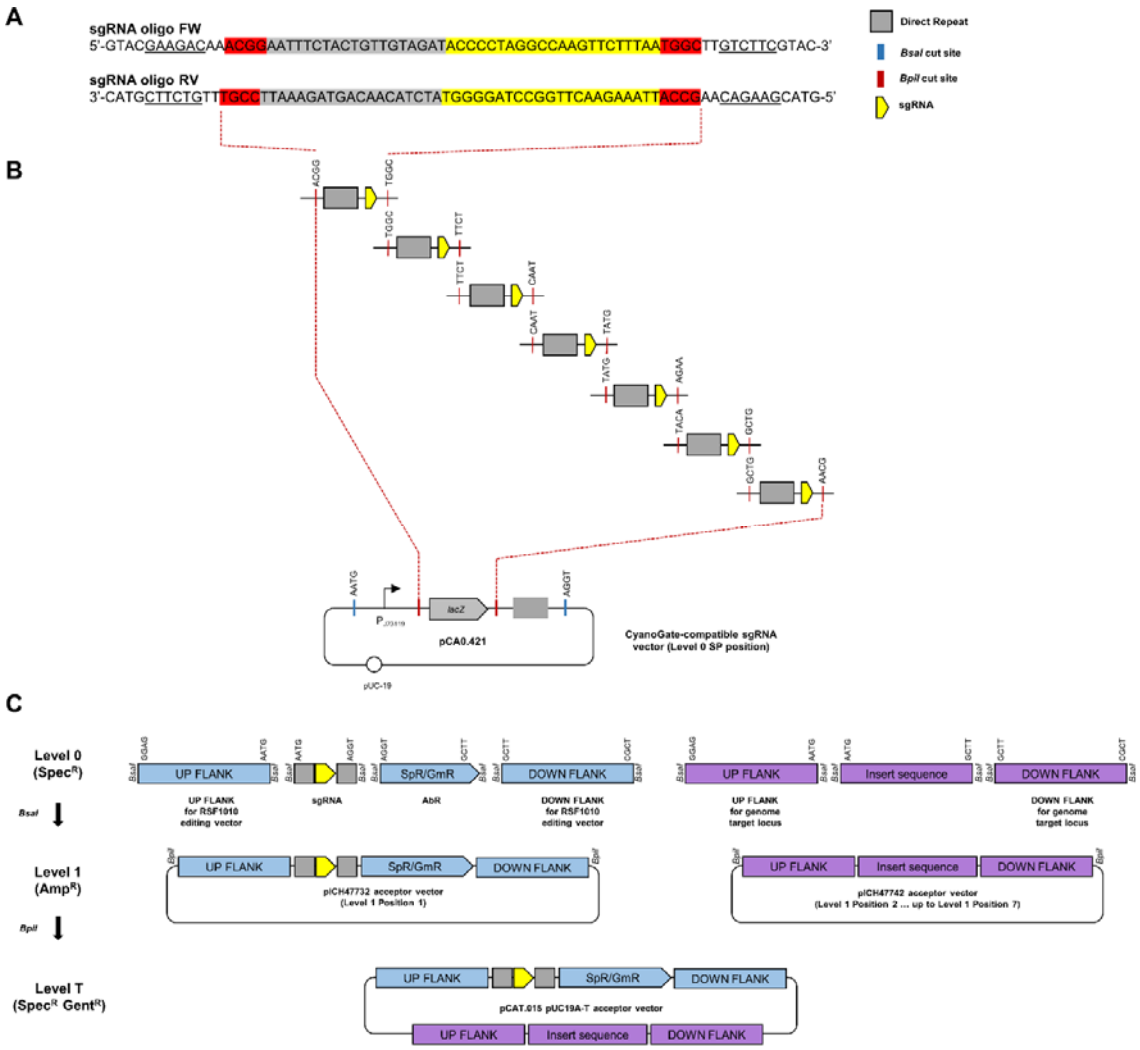

Assembly of sgRNA plasmid vectors (adapted from Liao et al., 2019)

1. To anneal oligonucleotides for making dsDNA parts for assembly (A), add 15 µL of the forward and reverse oligonucleotides into a PCR tube and incubate in a thermal cycler using the following step-down program: 95°C for 5 min, then decrease by 1°C incrementally and hold for 30 seconds for 79 cycles (until 25°C).
2. Level 0 assembly (B): In a PCR tube, add 2 µL of T4 ligation buffer, 2 µL of ATP (10 mM), 1 µL of each annealed repeat-spacer subunit (from 1.), 50 ng of the sgRNA acceptor vector (pCA0.421, Supplementary Table S1), 0.5 µL of T4 ligase, 1.5 µL of BpiI, and water to a total volume of 20 µL. Mix by pipetting and spin down briefly. Incubate the tube in a thermal cycler using the following program: 30 cycles of alternating digestion and ligation (37°C for 5 min, 16°C for 5 min) followed by a final digestion step (60°C for 5 min).
3. In a 1.5 mL microcentrifuge tube, transform 10 µL of the assembly reaction into 30 µl of competent TOP10 *E. coli* cells using the heat shock method. Add 500 µL LB to the cells and shake at 37°C for 1 h. Plate the cells in LB gar supplemented with 100 ug/mL spectinomycin and 40 ug/mL X-gal, and incubate overnight at 37 °C.
4. Screen the white colonies by colony PCR and Sanger sequencing.

Supplementary Figure S7. CRISPR-Cas12a double HR editing approach – sgRNA, repair template and hybrid suicide vector assembly. **(A)** sgRNA were assembled by annealing oligonucleotides incorporating the desired 18-22bp sgRNA (yellow), direct repeat (grey),

1360 unique 4 bp overhangs (red) and BpiI sites (underlined) for **(B)** assembly into the pC0.421
1361 sgRNA acceptor vector. Overhangs match those from the CRATES system and allow for
1362 assembly of an array of between one and seven sgRNAs (Liao et al., 2019). **(C)** MoClo
1363 assembly of level 0 parts into level 1 vectors and then a level T hybrid suicide vector
1364 incorporating the sgRNA(s) in position 1 and homology repair template(s) in position 2 up to
1365 position 7 using the available Plant MoClo level 1 acceptor vectors (Engler et al. 2014).
1366 Using this system between one and six genomic loci can be targeted simultaneously. A
1367 protocol for assembly of the sgRNA plasmid vectors is included.

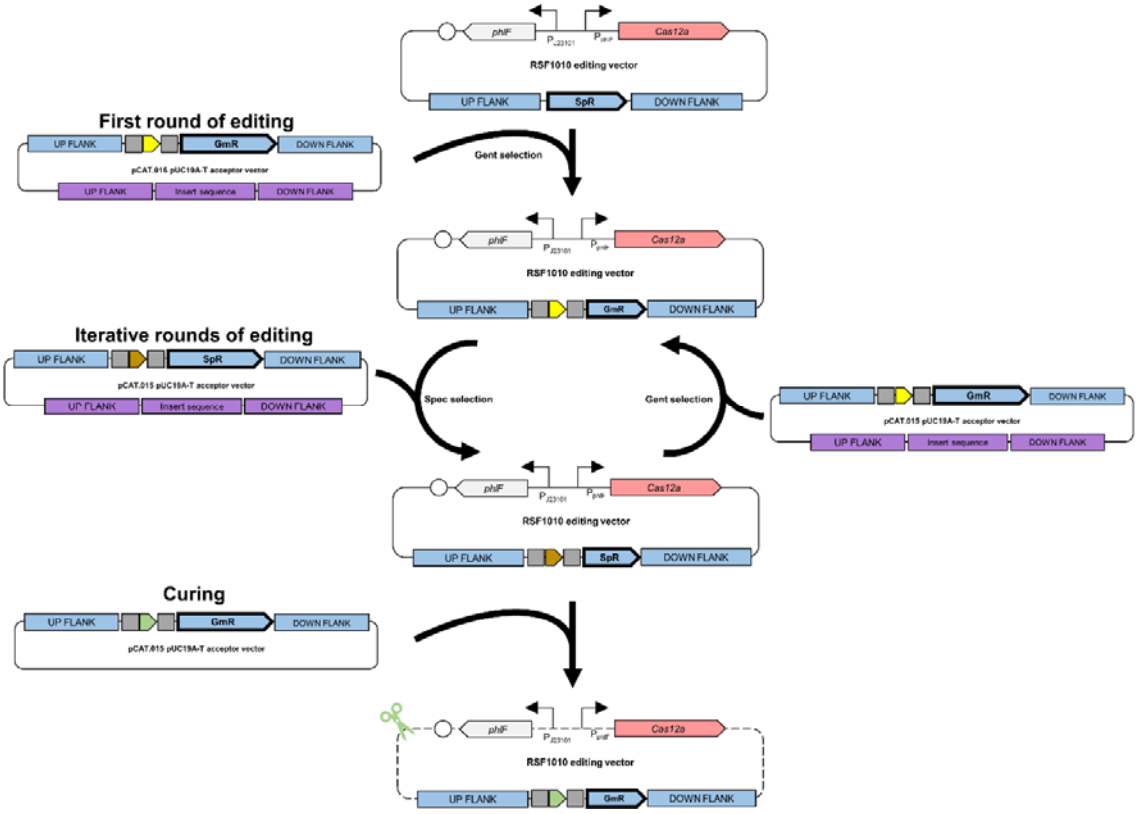

Protocol for transformation with hybrid suicide vectors

1. Grow the editing strain from OD_{750} = 0.2 to the initial stages of exponential growth (OD_{750} = ~0.8).
2. Centrifuge 1 mL of the editing strain for 10 min at 3,500 *g* and wash the cell pellet with fresh culture media three times to remove antibiotics.
3. Dilute the washed editing strain to OD_{750} = 0.2 and add 1.5 µg of purified hybrid suicide vector to 1 mL of the editing strain.
4. Incubate for 4 h at 30°C in 2% (v/v) CO_2 under warm white LED light (150 µmol photons m^{-2} s^{-1}) before adding 10 µM DAPG and continuing incubation overnight.
5. Plate the transformation mixture on to agar plates supplemented with appropriate antibiotics (25 µg mL^{-1} spectinomycin, 50 µg mL^{-1} gentamicin) and 10 µM DAPG and incubate as described in step 4.
6. Screen for mutant colonies using colony PCR.

Supplementary Figure S8. Pipeline for iterative CRISPR-Cas12a editing using the double HR approach. In the first round of editing the hybrid suicide vector recombines with the editing vector to introduce an sgRNA (or sgRNA array) and replaces the SpR with GmR for subsequent selection on gentamicin-supplemented agar plates (also see **Figure 6A**). Subsequent rounds of editing involved cycling between hybrid suicide vectors that exchange SpR and GmR for delivery of new sgRNA(s) to the editing vector. Curing the edited strain of the editing vector to generate a fully markerless strain is done using a hybrid suicide vector (e.g. pC1.530, **Supplementary Table S1**), which delivers a self-targeting sgRNA to the

1390 editing vector. A protocol for transformation with the hybrid suicide vector and induction
1391 with DAPG is included.
1392

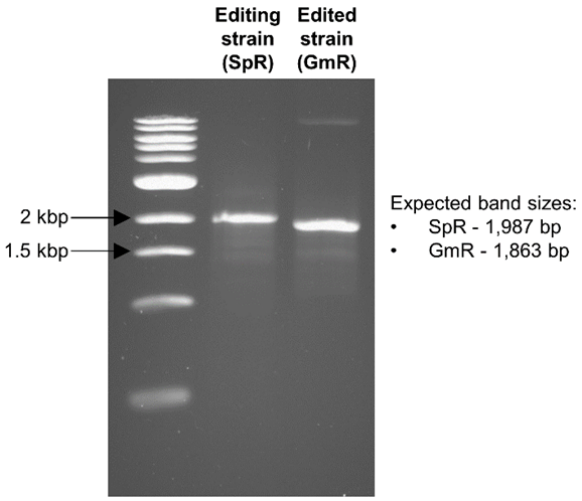

1393

1394 **Supplementary Figure S9.** Confirmation of recombination between the hybrid suicide
1395 vector and editing vector. Example colony PCR of a transformant showing replacement of
1396 SpR by GmR

1397

Parsed Citations

Abbas A, Morrissey JP, Marquez PC, Sheehan MM, Delany IR, O'Gara F (2002) Characterization of interactions between the transcriptional repressor PhlF and its binding site at the phlA promoter in Pseudomonas fluorescens F113. J Bacteriol 184: 3008–3016
Google Scholar: Author Only Title Only Author and Title

Bae S, Park J, Kim J-S (2014) Cas-OFFinder: a fast and versatile algorithm that searches for potential off-target sites of Cas9 RNA-guided endonucleases. Bioinformatics 30: 1473–1475
Google Scholar: Author Only Title Only Author and Title

Baldanta S, Guevara G, Navarro-Llorens JM (2022) SEVA-Cpf1, a CRISPR-Cas12a vector for genome editing in cyanobacteria. Microb Cell Factories 21: 103
Google Scholar: Author Only Title Only Author and Title

Batterton JC, Van Baalen C (1971) Growth responses of blue-green algae to sodium chloride concentration. Archiv Mikrobiol 76: 151–165
Google Scholar: Author Only Title Only Author and Title

Behle A, Saake P, Germann AT, Dienst D, Axmann IM (2020) Comparative dose–response analysis of inducible promoters in cyanobacteria. ACS Synth Biol 9: 843–855
Google Scholar: Author Only Title Only Author and Title

Behler J, Vijay D, Hess WR, Akhtar MK (2018) CRISPR-based technologies for metabolic engineering in cyanobacteria. Trends Biotechnol 36: 996–1010
Google Scholar: Author Only Title Only Author and Title

BEIS (2021) 'Net Zero Strategy: Build Back Greener'. Department for Business, Energy, and International Strategy. Available at: https://www.gov.uk/government/publications/net-zero-strategy (Accessed: 13 September 2022).
Google Scholar: Author Only Title Only Author and Title

Bernhards CB, Liem AT, Berk KL, Roth PA, Gibbons HS, Lux MW (2022) Putative phenotypically neutral genomic insertion points in prokaryotes. ACS Synth Biol 11: 1681–1685
Google Scholar: Author Only Title Only Author and Title

Bishé B, Taton A, Golden JW (2019) Modification of RSF1010-based broad-host-range plasmids for improved conjugation and cyanobacterial bioprospecting. iScience 20: 216–228
Google Scholar: Author Only Title Only Author and Title

Cameron JC, Pakrasi HB (2011) Glutathione facilitates antibiotic resistance and photosystem I stability during exposure to gentamicin in cyanobacteria. Appl Environ Microbiol 77: 3547–3550
Google Scholar: Author Only Title Only Author and Title

Cengic I, Cañadas IC, Minton NP, Hudson EP (2022) Inducible CRISPR/Cas9 allows for multiplexed and rapidly segregated single-target genome editing in Synechocystis sp. PCC 6803. ACS Synth Biol 11: 3100–3113
Google Scholar: Author Only Title Only Author and Title

Chen Y-J, Liu P, Nielsen AAK, Brophy JAN, Clancy K, Peterson T, Voigt CA (2013) Characterization of 582 natural and synthetic terminators and quantification of their design constraints. Nat Methods 10: 659–664
Google Scholar: Author Only Title Only Author and Title

Chi X, Zhang S, Sun H, Duan Y, Qiao C, Luan G, Lu X (2019) Adopting a theophylline-responsive riboswitch for flexible regulation and understanding of glycogen metabolism in synechococcus elongatus PCC 7942. Front Microbiol 10:
Google Scholar: Author Only Title Only Author and Title

Cho BA, Moreno-Cabezuelo JÁ, Mills LA, del Río Chanona EA, Lea-Smith DJ, Zhang D (2023) Integrated experimental and photo-mechanistic modelling of biomass and optical density production of fast versus slow growing model cyanobacteria. Algal Res 70: 102997
Google Scholar: Author Only Title Only Author and Title

Collias D, Vialetto E, Yu J, Co K, Almási É d H, Rüttiger A-S, Achmedov T, Strowig T, Beisel CL (2023) Systematically attenuating DNA targeting enables CRISPR-driven editing in bacteria. Nat Commun 14: 680
Google Scholar: Author Only Title Only Author and Title

Collier JL, Grossman AR (1994) A small polypeptide triggers complete degradation of light-harvesting phycobiliproteins in nutrient-deprived cyanobacteria. EMBO J 13: 1039–1047
Google Scholar: Author Only Title Only Author and Title

Dallo T, Krishnakumar R, Kolker SD, Ruffing AM (2023) High-Density Guide RNA Tiling and Machine Learning for Designing CRISPR Interference in Synechococcus sp. PCC 7002. ACS Synth Biol. doi: 10.1021/acssynbio.2c00653

Google Scholar: Author Only Title Only Author and Title

Daneshvar E, Wicker RJ, Show P-L, Bhatnagar A (2022) Biologically-mediated carbon capture and utilization by microalgae towards sustainable CO2 biofixation and biomass valorization – A review. Chem Eng J 427: 130884
Google Scholar: Author Only Title Only Author and Title

Depardieu F, Bikard D (2020) Gene silencing with CRISPRi in bacteria and optimization of dCas9 expression levels. Methods 172: 61–75
Google Scholar: Author Only Title Only Author and Title

Dias E, Oliveira M, Jones-Dias D, Vasconcelos V, Ferreira E, Manageiro V, Caniça M (2015) Assessing the antibiotic susceptibility of freshwater Cyanobacteria spp. Front Microbiol 6: 799
Google Scholar: Author Only Title Only Author and Title

Domínguez-Martín MA, Sauer PV, Kirst H, Sutter M, Bína D, Greber BJ, Nogales E, Polívka T, Kerfeld CA (2022) Structures of a phycobilisome in light-harvesting and photoprotected states. Nature 609: 835–845
Google Scholar: Author Only Title Only Author and Title

Engler C, Youles M, Gruetzner R, Ehnert T-M, Werner S, Jones JDG, Patron NJ, Marillonnet S (2014) A golden gate modular cloning toolbox for plants. ACS Synth Biol 3: 839–843
Google Scholar: Author Only Title Only Author and Title

Favrot L, Blanchard JS, Vergnolle O (2016) Bacterial GCN5-Related N-Acetyltransferases: From Resistance to Regulation. Biochemistry 55: 989–1002
Google Scholar: Author Only Title Only Author and Title

Fontana J, Dong C, Ham JY, Zalatan JG, Carothers JM (2018) Regulated expression of sgRNAs tunes CRISPRi in E. coli. Biotechnology Journal 13: 1800069
Google Scholar: Author Only Title Only Author and Title

Gale GAR, Schiavon Osorio AA, Mills LA, Wang B, Lea-Smith DJ, McCormick AJ (2019) Emerging species and genome editing tools: future prospects in cyanobacterial synthetic biology. Microorganisms 7: 409
Google Scholar: Author Only Title Only Author and Title

Gale GAR, Wang B, McCormick AJ (2021) Evaluation and comparison of the efficiency of transcription terminators in different cyanobacterial species. Front Microbiol 11:
Google Scholar: Author Only Title Only Author and Title

Goodchild-Michelman IM, Church GM, Schubert MG, Tang T-C (2023) Light and carbon: Synthetic biology toward new cyanobacteria-based living biomaterials. Mater Today Bio 19: 100583
Google Scholar: Author Only Title Only Author and Title

Gordon GC, Korosh TC, Cameron JC, Markley AL, Begemann MB, Pfleger BF (2016) CRISPR interference as a titratable, trans-acting regulatory tool for metabolic engineering in the cyanobacterium Synechococcus sp. strain PCC 7002. Metab Eng 38: 170–179
Google Scholar: Author Only Title Only Author and Title

Hitchcock A, Hunter CN, Canniffe DP (2020) Progress and challenges in engineering cyanobacteria as chassis for light-driven biotechnology. Microb Biotechnol 13: 363–367
Google Scholar: Author Only Title Only Author and Title

Huang H-H, Lindblad P (2013) Wide-dynamic-range promoters engineered for cyanobacteria. J Biol Eng 7: 10
Google Scholar: Author Only Title Only Author and Title

Iwai M, Katoh H, Katayama M, Ikeuchi M (2004) Improved genetic transformation of the thermophilic cyanobacterium, thermosynechococcus elongatus BP-1. Plant Cell Physiol 45: 171–175
Google Scholar: Author Only Title Only Author and Title

Jaiswal D, Sengupta A, Sengupta S, Madhu S, Pakrasi HB, Wangikar PP (2020) A novel cyanobacterium Synechococcus elongatus PCC11802 has distinct genomic and metabolomic characteristics compared to its neighbor PCC 11801. Sci Rep 10: 191
Google Scholar: Author Only Title Only Author and Title

Jaiswal D, Sengupta A, Sohoni S, Sengupta S, Phadnavis AG, Pakrasi HB, Wangikar PP (2018) Genome features and biochemical characteristics of a robust, fast growing and naturally transformable cyanobacterium Synechococcus elongatus PCC11801 isolated from India. Sci Rep 8: 16632
Google Scholar: Author Only Title Only Author and Title

Jester BW, Zhao H, Gewe M, Adame T, Perruzza L, Bolick DT, Agosti J, Khuong N, Kuestner R, Gamble C, et al (2022) Development of spirulina for the manufacture and oral delivery of protein therapeutics. Nat Biotechnol 40: 956–964
Google Scholar: Author Only Title Only Author and Title

Jones CM, Parrish S, Nielsen DR (2021) Exploiting polyploidy for markerless and plasmid-free genome engineering in cyanobacteria. ACS Synth Biol 10: 2371–2382
Google Scholar: Author Only Title Only Author and Title

Kavita K, Breaker RR (2023) Discovering riboswitches: the past and the future. Trends Biochem Sci 48: 119–141
Google Scholar: Author Only Title Only Author and Title

Kelly CL, Taylor GM, Hitchcock A, Torres-Méndez A, Heap JT (2018) A rhamnose-inducible system for precise and temporal control of gene expression in cyanobacteria. ACS Synth Biol 7: 1056–1066
Google Scholar: Author Only Title Only Author and Title

Khetkorn W, Incharoensakdi A, Lindblad P, Jantaro S (2016) Enhancement of poly-3-hydroxybutyrate production in Synechocystis sp. PCC 6803 by overexpression of its native biosynthetic genes. Bioresour Technol 214: 761–768
Google Scholar: Author Only Title Only Author and Title

Kopka J, Schmidt S, Dethloff F, Pade N, Berendt S, Schottkowski M, Martin N, Dühring U, Kuchmina E, Enke H, et al (2017) Systems analysis of ethanol production in the genetically engineered cyanobacterium Synechococcus sp. PCC 7002. Biotechnol Biofuels 10: 56
Google Scholar: Author Only Title Only Author and Title

Kufryk GI, Sachet M, Schmetterer G, Vermaas WFJ (2002) Transformation of the cyanobacterium Synechocystis sp. PCC 6803 as a tool for genetic mapping: optimization of efficiency. FEMS Microbiol Lett 206: 215–219
Google Scholar: Author Only Title Only Author and Title

Lauritsen I, Porse A, Sommer MOA, Nørholm MHH (2017) A versatile one-step CRISPR-Cas9 based approach to plasmid-curing. Microb Cell Factories 16: 135
Google Scholar: Author Only Title Only Author and Title

Lea-Smith DJ, Bombelli P, Dennis JS, Scott SA, Smith AG, Howe CJ (2014) Phycobilisome-deficient strains of Synechocystis sp. PCC 6803 have reduced size and require carbon-limiting conditions to exhibit enhanced productivity. Plant Physiol 165: 705–714
Google Scholar: Author Only Title Only Author and Title

Lea-Smith DJ, Summerfield TC, Ducat DC, Lu X, McCormick AJ, Purton S (2021) Editorial: Exploring the growing role of cyanobacteria in industrial biotechnology and sustainability. Front Microbiol 12:
Google Scholar: Author Only Title Only Author and Title

Lea-Smith DJ, Vasudevan R, Howe CJ (2016) Generation of marked and markerless mutants in model cyanobacterial species. J Vis Exp 54001
Google Scholar: Author Only Title Only Author and Title

Li H, Shen CR, Huang C-H, Sung L-Y, Wu M-Y, Hu Y-C (2016) CRISPR-Cas9 for the genome engineering of cyanobacteria and succinate production. Metab Eng 38: 293–302
Google Scholar: Author Only Title Only Author and Title

Li S, Sun T, Xu C, Chen L, Zhang W (2018) Development and optimization of genetic toolboxes for a fast-growing cyanobacterium Synechococcus elongatus UTEX 2973. Metab Eng 48: 163–174
Google Scholar: Author Only Title Only Author and Title

Liberton M, Chrisler WB, Nicora CD, Moore RJ, Smith RD, Koppenaal DW, Pakrasi HB, Jacobs JM (2017) Phycobilisome truncation causes widespread proteome changes in Synechocystis sp. PCC 6803. PLoS One 12: e0173251
Google Scholar: Author Only Title Only Author and Title

Lin P-C, Zhang F, Pakrasi HB (2021) Enhanced limonene production in a fast-growing cyanobacterium through combinatorial metabolic engineering. Metab Eng Commun 12: e00164
Google Scholar: Author Only Title Only Author and Title

Lindberg P, Park S, Melis A (2010) Engineering a platform for photosynthetic isoprene production in cyanobacteria, using Synechocystis as the model organism. Metab Eng 12: 70–79
Google Scholar: Author Only Title Only Author and Title

Liu D, Johnson VM, Pakrasi HB (2020) A reversibly induced CRISPRi system targeting photosystem II in the cyanobacterium Synechocystis sp. PCC 6803. ACS Synth Biol 9: 1441–1449
Google Scholar: Author Only Title Only Author and Title

Liu D, Pakrasi HB (2018) Exploring native genetic elements as plug-in tools for synthetic biology in the cyanobacterium Synechocystis sp. PCC 6803. Microb Cell Factories 17: 48
Google Scholar: Author Only Title Only Author and Title

Ma AT, Schmidt CM, Golden JW (2014) Regulation of gene expression in diverse cyanobacterial species by using theophylline-responsive riboswitches. Appl Environ Microbiol 80: 6704–6713

Google Scholar: Author Only Title Only Author and Title

Meyer AJ, Segall-Shapiro TH, Glassey E, Zhang J, Voigt CA (2019) Escherichia coli "Marionette" strains with 12 highly optimized small-molecule sensors. Nat Chem Biol 15: 196–204
Google Scholar: Author Only Title Only Author and Title

Meyer R (2009) Replication and conjugative mobilization of broad host-range IncQ plasmids. Plasmid 62: 57–70
Google Scholar: Author Only Title Only Author and Title

Miao R, Jahn M, Shabestary K, Hudson EP (2023) CRISPR interference screens reveal tradeoffs between growth rate and robustness in Synechocystis sp. PCC 6803 across trophic conditions. 2023.02.13.528328
Google Scholar: Author Only Title Only Author and Title

Mills LA, Moreno-Cabezuelo JÁ, Włodarczyk A, Victoria AJ, Mejías R, Nenninger A, Moxon S, Bombelli P, Selão TT, McCormick AJ, et al (2022) Development of a biotechnology platform for the fast-growing cyanobacterium Synechococcus sp. PCC 11901. Biomolecules 12: 872
Google Scholar: Author Only Title Only Author and Title

Mittermair S, Lakatos G, Nicoletti C, Ranglová K, Manoel JC, Grivalský T, Kozhan DM, Masojídek J, Richter J (2021) Impact of glgA1, glgA2 or glgC overexpression on growth and glycogen production in Synechocystis sp. PCC 6803. J Biotechnol 340: 47–56
Google Scholar: Author Only Title Only Author and Title

Nakahira Y, Ogawa A, Asano H, Oyama T, Tozawa Y (2013) Theophylline-dependent riboswitch as a novel genetic tool for strict regulation of protein expression in cyanobacterium synechococcus elongatus PCC 7942. Plant Cell Physiol 54: 1724–1735
Google Scholar: Author Only Title Only Author and Title

Ng AH, Berla BM, Pakrasi HB (2015) Fine-tuning of photoautotrophic protein production by combining promoters and neutral sites in the cyanobacterium Synechocystis sp. strain PCC 6803. Appl Environ Microbiol 81: 6857–6863
Google Scholar: Author Only Title Only Author and Title

Opel F, Siebert NA, Klatt S, Tüllinghoff A, Hantke JG, Toepel J, Bühler B, Nürnberg DJ, Klähn S (2022) Generation of synthetic shuttle vectors enabling modular genetic engineering of cyanobacteria. ACS Synth Biol 11: 1758–1771
Google Scholar: Author Only Title Only Author and Title

Pinto F, Pacheco CC, Oliveira P, Montagud A, Landels A, Couto N, Wright PC, Urchueguía JF, Tamagnini P (2015) Improving a Synechocystis-based photoautotrophic chassis through systematic genome mapping and validation of neutral sites. DNA Res 22: 425–437
Google Scholar: Author Only Title Only Author and Title

Porra RJ, Thompson WA, Kriedemann PE (1989) Determination of accurate extinction coefficients and simultaneous equations for assaying chlorophylls a and b extracted with four different solvents: verification of the concentration of chlorophyll standards by atomic absorption spectroscopy. Biochim Biophys Acta - Bioenerg 975: 384–394
Google Scholar: Author Only Title Only Author and Title

Puzorjov A, Dunn KE, McCormick AJ (2021) Production of thermostable phycocyanin in a mesophilic cyanobacterium. Metab Eng Commun 13: e00175
Google Scholar: Author Only Title Only Author and Title

Puzorjov A, McCormick AJ (2020) Phycobiliproteins from extreme environments and their potential applications. J Exp Bot 71: 3827–3842
Google Scholar: Author Only Title Only Author and Title

Puzorjov A, Mert Unal S, Wear MA, McCormick AJ (2022) Pilot scale production, extraction and purification of a thermostable phycocyanin from Synechocystis sp. PCC 6803. Bioresour Technol 345: 126459
Google Scholar: Author Only Title Only Author and Title

Racharaks R, Arnold W, Peccia J (2021) Development of CRISPR-Cas9 knock-in tools for free fatty acid production using the fast-growing cyanobacterial strain Synechococcus elongatus UTEX 2973. J Microbiol Methods 189: 106315
Google Scholar: Author Only Title Only Author and Title

Rautela A, Kumar S (2022) Engineering plant family TPS into cyanobacterial host for terpenoids production. Plant Cell Rep 41: 1791–1803
Google Scholar: Author Only Title Only Author and Title

Ruffing AM, Jensen TJ, Strickland LM (2016) Genetic tools for advancement of Synechococcus sp. PCC 7002 as a cyanobacterial chassis. Microb Cell Factories 15: 190
Google Scholar: Author Only Title Only Author and Title

Sakamoto T, Shen G, Higashi S, Murata N, Bryant DA (1997) Alteration of low-temperature susceptibility of the cyanobacterium Synechococcus sp. PCC 7002 by genetic manipulation of membrane lipid unsaturation. Arch Microbiol 169: 20–28
Google Scholar: Author Only Title Only Author and Title

Sakurai I, Stazic D, Eisenhut M, Vuorio E, Steglich C, Hess WR, Aro E-M (2012) Positive regulation of psbA gene expression by cis-encoded antisense RNAs in Synechocystis sp. PCC 6803. Plant Physiol 160: 1000–1010
Google Scholar: Author Only Title Only Author and Title

Santomartino R, Averesch NJH, Bhuiyan M, Cockell CS, Colangelo J, Gumulya Y, Lehner B, Lopez-Ayala I, McMahon S, Mohanty A, et al (2023) Toward sustainable space exploration: a roadmap for harnessing the power of microorganisms. Nat Commun 14: 1391
Google Scholar: Author Only Title Only Author and Title

Saveria T, Parthiban C, Seilie AM, Brady C, Martinez A, Manocha R, Afreen E, Zhao H, Krzeszowski A, Ferrara J, et al (2022) Needle-free, spirulina-produced Plasmodium falciparum circumsporozoite vaccination provides sterile protection against pre-erythrocytic malaria in mice. NPJ Vaccines 7: 1–11
Google Scholar: Author Only Title Only Author and Title

Selão TT (2022) Exploring cyanobacterial diversity for sustainable biotechnology. J Exp Bot 73: 3057–3071
Google Scholar: Author Only Title Only Author and Title

Sengupta A, Pritam P, Jaiswal D, Bandyopadhyay A, Pakrasi HB, Wangikar PP (2020a) Photosynthetic co-production of succinate and ethylene in a fast-growing cyanobacterium, Synechococcus elongatus PCC 11801. Metabolites 10: 250
Google Scholar: Author Only Title Only Author and Title

Sengupta S, Jaiswal D, Sengupta A, Shah S, Gadagkar S, Wangikar PP (2020b) Metabolic engineering of a fast-growing cyanobacterium Synechococcus elongatus PCC 11801 for photoautotrophic production of succinic acid. Biotechnol Biofuels 13: 89
Google Scholar: Author Only Title Only Author and Title

Shiraishi H, Nishida H (2022) Complete genome sequence of the edible filamentous cyanobacterium arthrospira platensis nies-39, based on long-read sequencing. Microbiol Resour Announc 12: e01139-22
Google Scholar: Author Only Title Only Author and Title

Soini J, Ukkonen K, Neubauer P (2008) High cell density media for Escherichia coli are generally designed for aerobic cultivations – consequences for large-scale bioprocesses and shake flask cultures. Microb Cell Factories 7: 26
Google Scholar: Author Only Title Only Author and Title

Su T, Liu F, Gu P, Jin H, Chang Y, Wang Q, Liang Q, Qi Q (2016) A CRISPR-Cas9 assisted non-homologous end-joining strategy for one-step engineering of bacterial genome. Sci Rep 6: 37895
Google Scholar: Author Only Title Only Author and Title

Taton A, Ma AT, Ota M, Golden SS, Golden JW (2017) NOT gate genetic circuits to control gene expression in cyanobacteria. ACS Synth Biol 6: 2175–2182
Google Scholar: Author Only Title Only Author and Title

Taton A, Unglaub F, Wright NE, Zeng WY, Paz-Yepes J, Brahamsha B, Palenik B, Peterson TC, Haerizadeh F, Golden SS, et al (2014) Broad-host-range vector system for synthetic biology and biotechnology in cyanobacteria. Nucleic Acids Res 42: e136
Google Scholar: Author Only Title Only Author and Title

Taylor GM, Hitchcock A, Heap JT (2021) Combinatorial assembly platform enabling engineering of genetically stable metabolic pathways in cyanobacteria. Nucleic Acids Res 49: e123
Google Scholar: Author Only Title Only Author and Title

Ungerer J, Pakrasi HB (2016) Cpf1 is a versatile tool for CRISPR genome editing across diverse species of cyanobacteria. Sci Rep 6: 39681
Google Scholar: Author Only Title Only Author and Title

Ungerer J, Wendt KE, Hendry JI, Maranas CD, Pakrasi HB (2018) Comparative genomics reveals the molecular determinants of rapid growth of the cyanobacterium Synechococcus elongatus UTEX 2973. Proc Natl Acad Sci USA 115: E11761–E11770
Google Scholar: Author Only Title Only Author and Title

Vasudevan R, Gale GAR, Schiavon AA, Puzorjov A, Malin J, Gillespie MD, Vavitsas K, Zulkower V, Wang B, Howe CJ, et al (2019) CyanoGate: a modular cloning suite for engineering cyanobacteria based on the plant MoClo syntax. Plant Physiol 180: 39–55
Google Scholar: Author Only Title Only Author and Title

Vento JM, Crook N, Beisel CL (2019) Barriers to genome editing with CRISPR in bacteria. J Ind Microbiol Biotechnol 46: 1327–1341
Google Scholar: Author Only Title Only Author and Title

Vogel AIM, Lale R, Hohmann-Marriott MF (2017) Streamlining recombination-mediated genetic engineering by validating three neutral integration sites in Synechococcus sp. PCC 7002. J Biol Eng 11: 19
Google Scholar: Author Only Title Only Author and Title

Wang S-Y, Li X, Wang S-G, Xia P-F (2023) Base editing for reprogramming cyanobacterium Synechococcus elongatus. Metab Eng 75: 91–99
Google Scholar: Author Only Title Only Author and Title

Wendt KE, Ungerer J, Cobb RE, Zhao H, Pakrasi HB (2016) CRISPR/Cas9 mediated targeted mutagenesis of the fast growing cyanobacterium Synechococcus elongatus UTEX 2973. Microb Cell Factories 15: 115
Google Scholar: Author Only Title Only Author and Title

Wilson KS, von Hippel PH (1995) Transcription termination at intrinsic terminators: the role of the RNA hairpin. Proc Natl Acad Sci USA 92: 8793–8797
Google Scholar: Author Only Title Only Author and Title

Włodarczyk A, Selão TT, Norling B, Nixon PJ (2020) Newly discovered Synechococcus sp. PCC 11901 is a robust cyanobacterial strain for high biomass production. Commun Biol 3: 1–14
Google Scholar: Author Only Title Only Author and Title

Xiao K, Yue X-H, Chen W-C, Zhou X-R, Wang L, Xu L, Huang F-H, Wan X (2018) Metabolic engineering for enhanced medium chain omega hydroxy fatty acid production in Escherichia coli. Front Microbiol 9: 139
Google Scholar: Author Only Title Only Author and Title

Yao L, Shabestary K, Björk SM, Asplund-Samuelsson J, Joensson HN, Jahn M, Hudson EP (2020) Pooled CRISPRi screening of the cyanobacterium Synechocystis sp PCC 6803 for enhanced industrial phenotypes. Nat Commun 11: 1666
Google Scholar: Author Only Title Only Author and Title

Yu J, Liberton M, Cliften PF, Head RD, Jacobs JM, Smith RD, Koppenaal DW, Brand JJ, Pakrasi HB (2015) Synechococcus elongatus UTEX 2973, a fast growing cyanobacterial chassis for biosynthesis using light and CO2. Sci Rep 5: 8132
Google Scholar: Author Only Title Only Author and Title

Zavřel T, Chmelík D, Sinetova MA, Červený J (2018) Spectrophotometric determination of phycobiliprotein content in cyanobacterium Synechocystis. J Vis Exp 58076
Google Scholar: Author Only Title Only Author and Title

Zess EK, Begemann MB, Pfleger BF (2016) Construction of new synthetic biology tools for the control of gene expression in the cyanobacterium Synechococcus sp. strain PCC 7002. Biotechnol Bioeng 113: 424–432
Google Scholar: Author Only Title Only Author and Title

Zetsche B, Gootenberg JS, Abudayyeh OO, Slaymaker IM, Makarova KS, Essletzbichler P, Volz SE, Joung J, van der Oost J, Regev A, et al (2015) Cpf1 is a single RNA-guided endonuclease of a class 2 CRISPR-Cas system. Cell 163: 759–771
Google Scholar: Author Only Title Only Author and Title

Zhang A, Carroll AL, Atsumi S (2017) Carbon recycling by cyanobacteria: improving CO2 fixation through chemical production. FEMS Microbiol Lett 364: fnx165
Google Scholar: Author Only Title Only Author and Title

Zhou Y, Sun T, Chen Z, Song X, Chen L, Zhang W (2019) Development of a new biocontainment strategy in model cyanobacterium Synechococcus strains. ACS Synth Biol 8: 2576–2584
Google Scholar: Author Only Title Only Author and Title